The development of oxygen content in the Greenland Sea from 1993 to 2008.

A study of convection depth and deep layer changes

Master in Chemical Oceanography

UNIVERSITY OF BERGEN
GEOPHYSICAL INSTITUTE

Helle Augdal Botnen

25^{th} of May 2009

Acknowledgement

Først og fremst vil jeg si takk til Eva Falck som har vært min veileder under arbeidet med masteroppgaven. Jeg har lært utrolig mye gjennom dette arbeidet og setter stor pris på alle tips og råd jeg har fått av deg. En stor takk også for at jeg fikk muligheten til å bli med deg på tokt. Det har vært en utrolig opplevelse og en god erfaring som jeg vil ta med meg videre.

Så vil jeg gjerne takke gjengen på Odd for godt samhold og god hjelp. Marianne, jeg tror vi begge har lært at caption i tabeller må stå før og ikke etter selve tabellen.. :-)

Takk til Geofysisk Institutt for muligheten til å dra på EGU konferansen i Wien. Det var en veldig god erfaring som ga mersmak på å jobbe videre innen forskning. Og da selvfølgelig innen oseanografien!!

Finally I would like to give a special thanks to Gereon Budéus. Thank you very much for the opportuinity to participate on the cruises with Merian and Polarstern. Both cruises were amazing and I appreciate very much this experience.

Helle Augdal Botnen, 25/05-09

Contents

Chapter 1

Introduction

1.1 Historical perspective on the Greenland Sea

The Greenland Sea is one of the few areas in the World Ocean where open ocean convection takes place. Together with the Laborador Sea, the Weddell Sea, and the Ross Sea, the Greenland Sea is an area of dense water formation through deep convection (e.g., Wadhams et al., 2002). These four areas consist of only a fraction of the global ocean, but are the areas where the densest water is produced. The dense water is of great importance due to its contribution to the thermohaline circulation as submerged bottom and deep currents bringing newly ventilated water from the poles. The dense water formed in the Greenland Sea flows south over the Greenland-Scotland Ridge through the Denmark Strait and contribute to the North Atlantic Deep Water as a part of the dense overflow water from the Nordic Seas (Greenland, Norwegian, and Iceland Seas).

Open ocean convection can be a result of many different physical conditions and mechanisms. It was early pointed out that the hydrography in the Greenland Sea was of such a character that complete overturning of the water column was thought to be the reason for deep water formation. This was first suggested by Mohn in 1887 and then further developed by Nansen and Helland-Hansen in 1909. Their suggestion of complete overturning should produce a homogeneous vertical structure in the Greenland Sea.

The first scientific observations in the Greenland Sea was made by H. Mohn and G.O. Sars in 1876 during the Norwegian North Atlantic Expedition. An important observation made during this expedition was the discovery of the shallow stratification followed by the nearly homogeneous water column in the central Greenland Sea. Further expeditions in this area were conducted by Helland-Hansen and Nansen. During their cruises to the Nordic Seas in the period from 1900 to 1904 they collected large amounts of scientific data. In 1909 they published their work "The Norwegian Sea" giving a description of the Iceland Sea, the Norwegian Sea, and the Greenland Sea based on data from the years 1900 to 1904. When mapping the bathymetry and describing the water masses in these seas they discovered a distinct feature. Helland-Hansen and Nansen claimed to have discovered a nearly uniform water mass that covered large parts of the Greenland, Norwegian, and Iceland Sea. During further investigations they found that this uniform water ascended close to

the surface in the Greenland Sea. The favourable cyclonic feature in this area contributed to low horizontal water fluxes that constrained the exchange of water and made it possible for the isopycnals to rise towards the surface. During the winter the uniform water ascends close to the surface pushing up the isopycnals leading to a shallow stratified surface layer which gets cooled due to heat loss from the surface to the atmosphere. This heat loss to the atmosphere will cause a densification of the surface layer that lead to a deteriation of the stratification making complete overturning possible. The produced "winter water" was carried down by active vertical circulation through the water column of nearly uniform density.
This was one of the early descriptions of the vertical convection taking place in the Greenland Sea producing dense bottom water. Helland-Hansen and Nansen (1909, p.324) stated that "the formation of cold, heavy bottom water was here directly observed on the very sea surface, as was previously expected, and the question of the process of its formation is thus finally settled beyond all doubt". However, there have not been any direct observations of convective events, and therefore questions have been risen whether or not the process described by Helland-Hansen and Nansen is correct.
In 1955 Metcalf also suggested that the convection in the Greenland Sea was a result of isopycnal doming, but he proposed that the large scale cooling of the surface layer was followed by sinking of the dense water along slighlty inclined isopycnals. This would produce the dense deep and bottom water observed in the Greenland Basin. Also Carmack and Aagaard (1973) suggested that the "deep water is formed by the cooling of surface water during winter primarily in the Greenland Gyre where the vertical stability prior to the onset of winter is minimal. The water sinks below the surface and is replaced from below by warmer water with a slightly higher salinity. As the cooling continues, the entire water column is progressively overturned until homogenity is obtained throughout."
The theory that deep and bottom water formation in the Greenland Sea is due to deep convection has been the major theory and that the cyclonic circulation in the Greenland Sea is an important precondition for a deep convection to be able to take place.

1.2 Motivation

The hydrographic structure and convective events in the Greenland Sea have been investigated since the late 1800s (Mohn, 1887). In recent years the reduction of deep convection and the following lack of deep water formation have been investigated (e.g., Schlosser et al. 1990). To better understand the behaviour of the convective events in the Greenland Sea on annual basis and over several years identification of the convection depth and processes that triggers convection are of great interest. Thereby it may be possible to state if the changes in the Greenland Sea water masses are part of an oscillating system like the North Atlantic Ocillation (Dicksson, 1996). The reduced production of deep water in later years causes changes in the hydrographic structure of the Greenland Sea. Since the water masses in the Norwegian and Iceland Seas have the Greenland Sea Deep Water as a parent water mass changes in the deep water formation may lead to changes in the hydrographic structure of

these seas (Blindheim and Rey, 2004). The changes in the hydrographic structure can also be seen in the density structure (Østerhus and Gammelsrød, 1999), and density changes in the different basins may further cause changes in the current directions. The difference in density between the deep waters of the Greenland and the Norwegian Basins have become smaller due to the lacking deep convection, and hence Greenland Sea Deep Water formation. This has probably caused the monitored reduction and change of current direction in the Jan Mayen Channel (Østerhus and Gammelsrød, 1999). The hydrographic changes in the Greenland Sea influences the hydrography of the entire Nordic Seas, and may therefore cause changes also in the North Atlantic Deep Water.

To gain more insight into these questions the purpose of this work is to use oxygen measurements from the Greenland Sea to conduct a historical study of possible changes in the oxygen content in the Greenland Sea and to investigate the possibility of using oxygen as an indicator for convection depth. In recent years it has been common to use an oxygen sensor mounted on the CTD to measure the oxygen concentration in the ocean. This gives a much more detalied profile than can be obtained by the Winkler method. Still the most accurate way to measure oxygen concentration is by the Winkler titration method that has been in use since 1888, but it is labour intensive and time consuming. However, the oxygen sensor data have to be calibrated to make sure they have the correct oxygen concentration. An attempt to find a method for correction of the sensor data by using the Winkler data has been conducted in Chapter 4. Unfortunaly this proved to be a much too tedious task and too time consuming for this work.

The developement of the oxygen concentent in the Greenland Sea, along with the temperature and salinity, have been investigated for the years from 1993 to 2008. Previous investigations of convection depth have been conducted by the use of temperature and salinity profiles intersecting the Greenland Basin (Karstensen et al., 2004; Ronski and Budéus, 2005). These variables can give a good indication of the convection type and hence the convection depth, however, some years give inconclusive results. Due to this it is desirable to identify another variable that can indicate the convection type when temperature and salinity fail to do so, and thus making it difficult to identify the convection depth (Ronski and Budéus, 2005). Oxygen concentration, which can only increase by influx at the sea surface, is thought to be a possible variable for identification of convection depth and this has been looked into. Finally, to give an impression of the concequences of the reduced deep convection investigation of the oxygen content in the deep layer of the Greenland Sea, below the convection depth, has been done. This to determine if any trend is present in the oxygen content, and to compare this with the changes in temperature, and salinity. The results from investigations of these aspects are presented in Chapter 5 and discussed in Chapter 6.

Chapter 2

The Greenland Sea

2.1 Bathymetry

The Greenland Sea, together with the Norwegian Sea and the Iceland Sea, are all situated south of the Arctic Ocean. The Greenland Sea is situated between 71° and 80° North, and between 20° West and 12° East. The bathymetry of the Greenland Sea is divided into two basins, the northern Boreas Basin and the southern Greenland Basin. The basins are both deep, reaching down to 3200-3800 meters at the deepest, and are surrounded by ridges and continental shelves. The ridges, that rise up to 2000-2500 meters depth, restrict the water mass exchange between the Greenland Sea and the Norwegian and Iceland Seas.
The smallest of the two basins, the Boreas Basin, is closed by the Fram Strait and Svalbard in the north, the Knipovich ridge in the east, Greenland in the west, and the Greenland Fracture Zone in the south. The Greenland Basin is closed by the Greenland Fracture Zone in the north, the Mohn ridge in the east, Greenland in the west, Jan Mayen, and the Jan Mayen Fracture Zone in the south. Along the Jan Mayen Fracture Zone runs a channel, the Jan Mayen Channel, which is the deepest passage in the Mohn Ridge, between the Greenland Sea and the Norwegian Sea. The maximum depth of the Greenland Sea is 3800 meters and is located in the Greenland Basin. The Boreas Basin has a maximum depth of 3200 meters. The Greenland Sea Gyre is located in the Greenland Basin and covers an area of approximatly 9×10^5 km^2, that gives a volume of 1.35×10^{15} m^3.

2.2 Hydrography

To be able to understand and describe the physical features in the Greenland Sea, such as convection, it is necessary to have an overview of the hydrography. Open ocean convection depends much on the hydrography because it is only under certain condition it can take place. The Greenland Sea is divided into three domaines, the Polar domain, the Arctic domain and the Atlantic domain. These domains are separated by the Polar and the Arctic Fronts where the Polar Front is located near the continetal shelf of Greenland and the Arctic Front is more or less fixated above the Mohn ridge. The Polar domain is located between Greenland and the Polar Front, the Arctic domain is located between the Polar and Arctic Front, and the

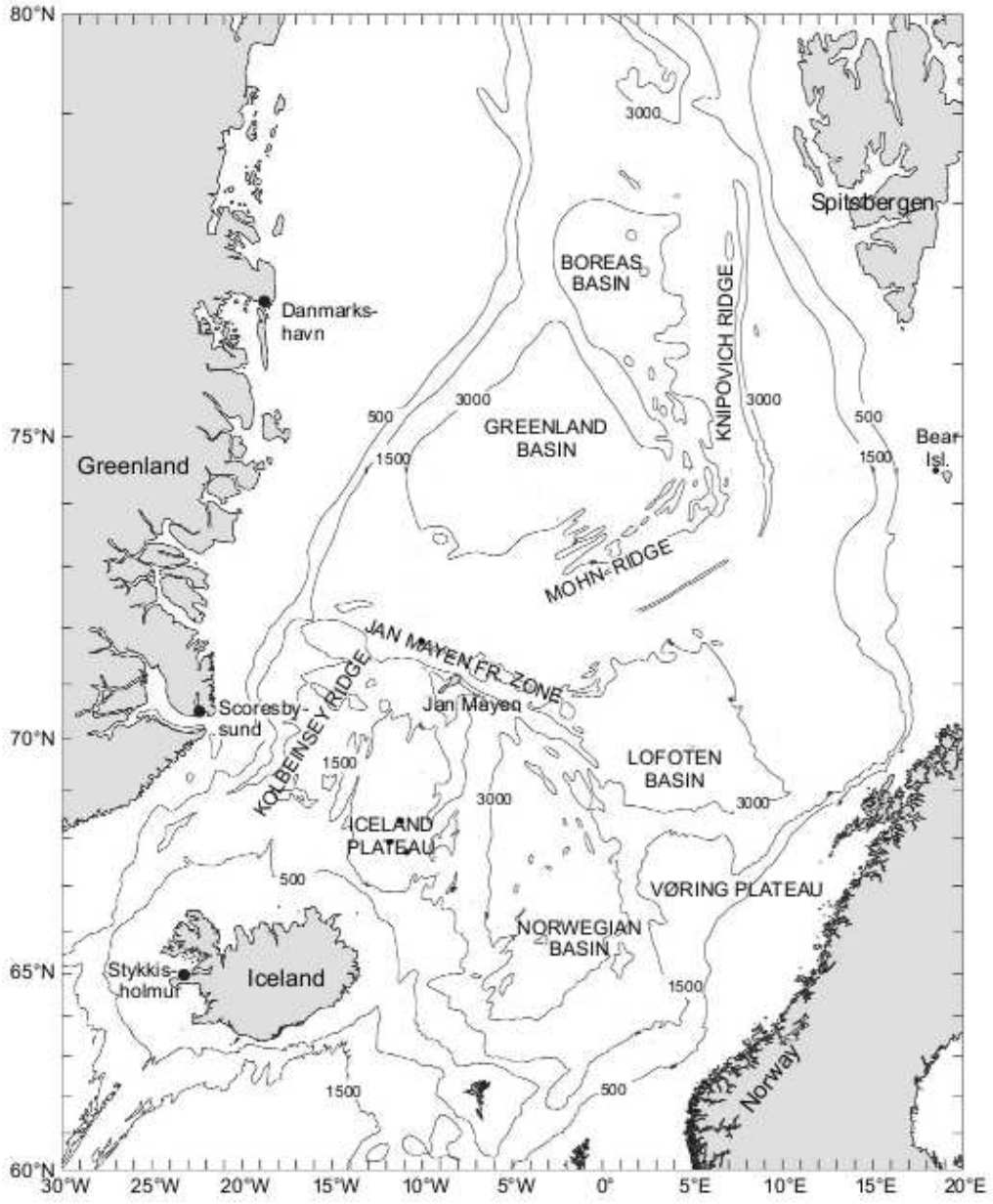

Figure 2.1: The bathymetry of the Greenland Sea (from Blindheim and Rey, 2004)

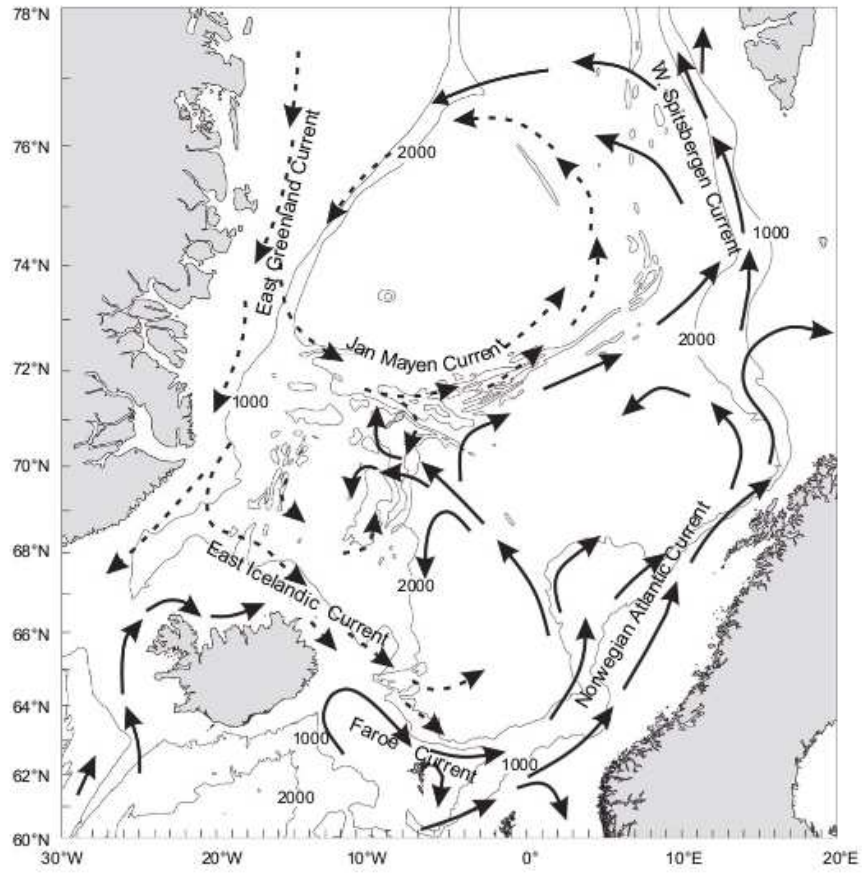

Figure 2.2: Currents in the Greenland Sea (from Blindheim and Rey, 2004)

Atlantic domain is located east of the Arctic Front. The reason for dividing the Greenland Sea into these domains are due to the location of the different water masses present. The Polar domain is dominated by water masses of polar origin, while the Atlantic domain is dominated by water of Atlantic origin. The Arctic domain is dominated by water that is a mix or modification of water from the Polar and Atlantic domains.
The fronts can be identified by strong horizontal temperature and salinity gradients at the surface which divides the Polar Surface Water in the East Greenland Current from the Arctic Surface Water in the Greenland Sea Gyre.

2.2.1 Currents

The currents in the Greenland Sea is of major importance for the cyclonic circulation in the upper layer of the Greenland Gyre. This circulation makes it possible for a vertical structure that favours deep convection.

The Norwegian Atlantic Current (NwAC) is the northern extention of the North Atlantic Current and the Gulf Stream, bringing warm and saline water from the Atlantic Ocean to the Norwegian Sea and the Greenland Sea. It flows into

the Norwegian Sea through the Faeroe-Shetland Channel and follows the coast of Norway. At the northern tip of Norway the NwAC is divided into two branches. One of these branches heads east into the Barents Sea while the other, the West Spitsbergen Current, continues north along Svalbard.

The West Spitsbergen Current (WSC) brings the warm Atlantic Water towards the Arctic Ocean. Part of this current heads into the Arctic Ocean north of Svalbard where it submerges to an intermediate layer, while the rest recirculates in the Fram Strait and contributes to the Return Atlantic Current.

The Return Atlantic Current (RAC) flows southwards underneath the Polar Water, in the East Greenland Current, at a depth between 200-800 meters and carries the Atlantic Water that has circulated around the Arctic Ocean or recirculated in the Fram Strait.

The East Greenland Current (EGC) streams south along the east coast of Greenland, bringing Polar Water and ice from the Arctic Ocean. Close to the Jan Mayen Fraction Zone a part of the EGC is deflected towards east and follows the southern edge of the Greenland Basin. This current is known as the Jan Mayen Current. The rest of the EGC continues southwards to the Denmark Strait and flows out into the Atlantic. Before it reaches the Denmark Strait another branch is deflected from the EGC, flowing south-east, known as the East Icelandic Current.

The Jan Mayen Current (JMC) is formed by a decflected branch from the EGC and flows eastwards along the Jan Mayen Fracture Zone along the souther rim of the Greenland Sea Gyre. The JMC is often considered the eastern extention of the EGC and is of importance due to its low salinity and temperature in the surface which favours ice formation and may advect fresh water into the Greenland Sea. When ice forms in the JMC this feature is known as "'Odden"' and may influences the convection in the Greenland Sea (Wilkinson and Wadhams, 2003).

The Greenland Sea Gyre The interactions and combination of these different currents form what is known as the Greenland Sea Gyre. The northward flowing WSC, the westwards flowing deflection of the WSC, the southward flowing EGC and the eastward flowing JMC contributes to the cyclonic circulation of the Greenland Sea Gyre. Mixing between the Atlantic and the Polar Water, forming the Arctic Water, is the reason for the high surface water densities in the Greenland Sea. High surface density favours convection, due to the possibility of an unstable surface layer.

2.2.2 Water masses

The Greenland Sea consists of different water masses coming from the Atlantic and the Arctic Ocean, and those water masses that are formed or modified in the Greenland Sea. A short decription of the main water masses in the Greenland Sea is given below.

Polar Water (PW) is found in the western part of the Greenland Sea and consists of water from the Arctic Ocean carried south by the EGC. It is characterised by low and variable salinity due to ice melting and contribution from Arctic Ocean Surface Water and extends from the surface down to 150-200 meters.

Arctic Water is a mixture of Atlantic and Polar Water and is found in the central Greenland Sea. The Arctic Water is generally divided into two slightly different water masses, the Arctic Surface Water (ASW) and the Arctic Intermediate Water (AIW). The ASW dominates the surface water in the Greenland Sea, between the Arctic and the Polar Front, while the AIW is found at intermediate depth. The major impact on the Greenland Sea is the effect they have as low salinity waters.

Atlantic Water (AW) is found in the eastern part of the Greenland Sea and is characterized by high temperature and salinity. This is water brought north by the NwAC and enters the Greenland Sea through the WSC. The Return Atlantic Water (RAW) is of Atlantic origin that has circulated into the EGC from the WSC and the Atlantic layer in the Arctic Ocean and is found below the PW in the western part of the Greenland Sea. It is the only water mass on the western side with temperature above zero and can therefore be easily identified.

The Arctic Ocean Deep Water (AODW) is the deep water entering the Greenland Sea from the Arctic Ocean. This water mass can be divided into two different water masses, Eurasian Basin Deep Water (EBDW) and Canadian Basin Deep Water (CBDW), where the EBDW has slightly lower temperatures than the CBDW. Both enter the Greenland Sea along the Greenland Slope in the Fram Strait, where the CBDW enters at depths above the EBDW.

The Greenland Sea Deep Water (GSDW) is found in the deeper parts of the Greenland Sea. This is colder and less saline than the AODW. It was formed by deep convection and used to fill the larger parts of the Greenland Basin, but lately it has been modified by mixing with AODW (e.g. Aagaard et al., 1991).

The Norwegian Sea Deep Water (NSDW) is produced by mixing of GSDW and EBDW and fills the deeper parts of the Norwegian Sea and flows towards the Arctic Ocean below the WSC.
For more detailes on the water masses it is refered to Blindheim and Østerhus (2005).

The different water masses can be identified by their temperature and salinity values and the ones that will be considered in this work are listed in Table 2.1.

Table 2.1: Water mass characteristics (from Schlichtholz and Houssais, 2002).

Acronym[1]	**Temperature**	**Salinity**
AIW	-1.1°C $< \theta <$ -0.5°C	34.7 < S < 34.9
	-0.8°C $< \theta <$ 0°C	34.9 $< S <$ 34.92[2]
NSDWw	-0.8°C $< \theta <$ -0.5°C	34.9 < S < 34.92[3]
	-0.5°C $< \theta <$ 0°C	34.9 < S < 34.92[4]
CBDW	-0.8°C $< \theta <$ -0.5°C	S > 34.92
NSDWc	-1.1°C $< \theta <$ -0.8°C	34.9 < S < 34.92
EBDW	-1.1°C $< \theta <$ -0.8°C	S > 34.92
GSDW	$\theta <$ -1.1°C	34.7 < S < 34.92

[1]AIW- Arctic Intermediate Water, NSDWw- warm Norwegian Sea Deep Water, CBDW- Canadian Basin Deep Water, NSDWc- cold Norwegian Sea Deep Water, EBDW- Eurasian Basin Deep Water, GSDW- Greenland Sea Deep Water; [2]if a salinity maximum is found in the range -1.1°C $< \theta <$ -0.5°C, 34.7 < S < 34.9; [3]if not AIW; [4]if not AIW

2.2.3 Vertical structure of the hydrography in the Greenland Sea

The classical view with the main feature being a dome shape in the middle of the Greenland Basin surrounded by the currents (Fig.2.3a) dates back to Nansen and Helland-Hansen (1909). Since the early 1990s a distinct stratification at intermediate water depth containing a temperature maximum, T_{max}, combined with increased salinity and a density gradient dominates the water structure (Fig. 2.3b). The strong vertical gradient in density present at the base of the T_{max} indicates a separation of water from past convective events and recent ventilation. Above the T_{max} there is today an intermediate layer, reaching from the surface layer and down to the density gradient, which is belived not to be in any contact with the deep waters below. The upper surface layer is influenced by the seasonal variations and cycles in heat and freshwater fluxes, but also lateral fluxes from the gyre rim (Ronski and Budéus, 2005a). The characteristics of the intermediate layer can experience annual changes depending on the strength of the winter convection. Below the T_{max} the deep water is quite homogenous especially in the centre of the gyre (Karstensen et al., 2005).

2.2.4 Physical mechanisms behind convection

As has already been mentioned different theories on how the deep water in the Greenland Sea is produced have been put forth over the years. For a deep convection to take place a cyclonic circulation is thought to be an important precondition (Helland-Hansen and Nansen, 1909; Metcalf, 1955), due to the resulting doming of the isopycnals lifting them closer to the surface in the centre of the gyre. This produces a nearly homogenous water structure below a shallow surface layer, which can cool and mix during winter, breaking down the stratification and give rise to a complete overturning of the water column. There have not been a direct observation of such an event and this has given reason to consider other physical mechanisms as

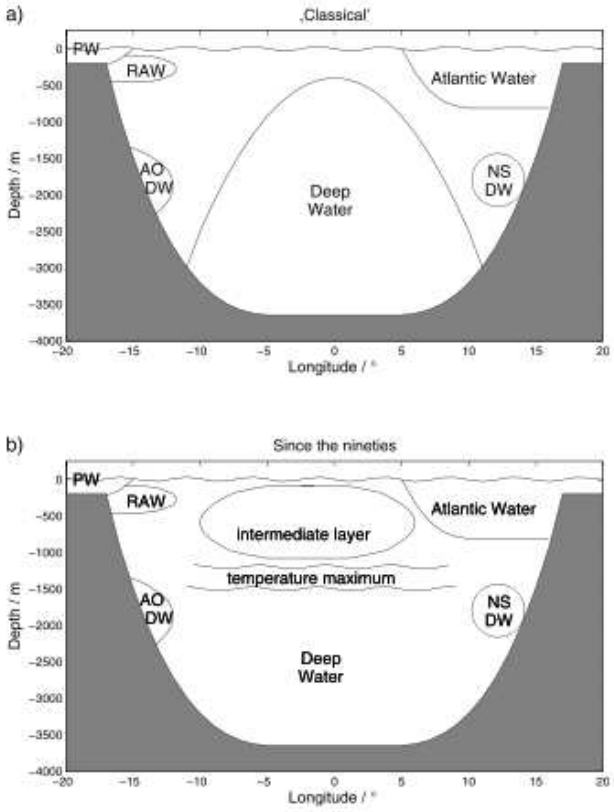

Figure 2.3: The modern and classical view of the vertical structure (from Ronski & Budéus, 2005a).

well.

Two plausible deepening processes are described by Aagaard and Carmack (1989) where one is based on progressive mixing of the surface layer and the other on the thermobaric effect (Fig. 2.4). Both are triggered by heat loss to the atmosphere and the following cooling of the surface. In case the surface water is more saline than the lower layers, cooling will make the surface water as dense as the lower layers at a temperature t2. At near-bottom pressure the deeper layers which will however be denser than the cooled surface water and therefore further cooling, to temperature t3, is necessary to drive the convection deeper. If the surface water is less saline than the deeper water and the surface water is cooled to the temperature making it as dense as the deep water, it has already passed the density of lower layers at all depths due to the thermobaric effect making the cold water denser as it sinks. Therefore it will continue to sink as a plume of dense water instead of a progressive deepening as in the first case. These deepening processes are called mixed layer deepening and plume convection, respectively.

Double-diffusion and caballing are other mechanisms thought to be responsible for deep convection (Aagaard and Carmack, 1989; Clarke et al., 1990). Clarke et al. (1990) interpreted the salinity-temperature maxima in the upper and deeper layers of the Greenland Sea as originating from a core of Atlantic Water coming from the Norwegian Sea getting colder, fresher, and denser, due to cross-isopycnal mixing, as

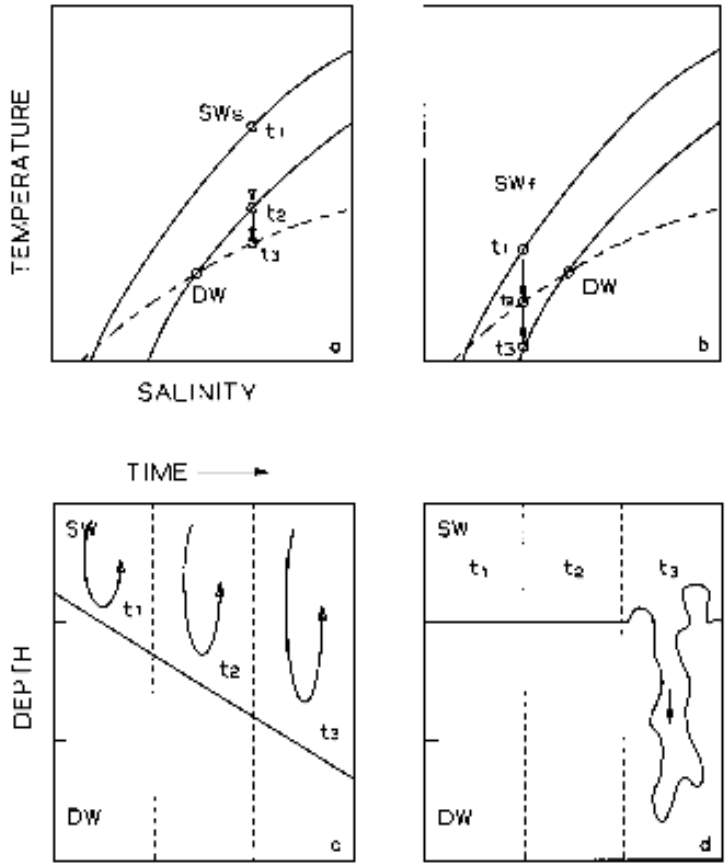

Figure 2.4: Schemes showing the basis for progressive mixing and plume convection (from Aagaard and Carmack, 1989)

it moves towards the centre of Greenland Sea gyre and eventually transforms into GSDW. This cooling and freshening are thought to be a result of double-diffusion between the water masses originally in the Greenland Sea and the inflowing Atlantic water. When the temperature-salinity maximum was formed around the outskirts of the Greenland Gyre, double-diffusion would result in a core layer extending into the gyre. Since heat exchanges more efficiently than salt, the core gets cooled and becomes denser than the surrounding warmer water. This leads to a weak circulation pattern that moves water down the axis of the core, which continues as long as the temperature in the core layer remains warmer than the water above it.
Concidering the different mechanisms for convection the theory based on the thermobaric effect and progressive mixing seems more reasonable than the others theories. According to the findings of Ronski and Budéus (2005) some years show progressive mixing, which they call mixed layer deepening, and some years are influenced by the thermobaric effect, which they call plume convection.

2.3 Oxygen

When studying dissolved oxygen, hereafter refered to as oxygen, in the ocean one have to concider the different sources and sinks. Sources for oxygen are gas transfer

from the atmosphere and biological production during photosynthesis in the upper surface layer where sunlight is available. Sinks are gas transfer from the ocean to the atmosphere, and respiration and remineralization by animals and bacteria throughout the water column. A continuous exchange of oxygen between the ocean and atmosphere takes place. The ability of sea water to dissolve oxygen is dependent on temperature, salinity, and the oxygen partial pressure. The solubility increases with partial pressure and diminishes with increasing temperature and salinity, which means that cold water can dissolve more oxygen than warm water.
The ocean's content of dissolved oxygen is a result of a dynamical balance between processes that consume oxygen and processes that produce oxygen (Gytre, 2004). Also the biological production and reduction of oxygen is assumed to be of the same annual magnitude (Broecker and Peng, 1982).
Based on this knowledge it is understandable that the longer a water mass is isolated from the surface the lower will the oxygen concentration become. By using this knowledge it is possible to estimate the age of a water mass, meaning, the time since the water mass last was present at the surface. Consequently this makes it possible to use oxygen as a tracer for ocean circulation. A high concentration of dissolved oxygen indicates water which has recently been in contact with the atmosphere whereas a low concentration indicates water that has been isolated for a period of time. To establish how long it has been since the water mass was at the surface it is necessary to know the oxygen concentration the water had before it departed from the surface (Broecker and Peng, 1982; Sarmiento and Gruber, 2006).

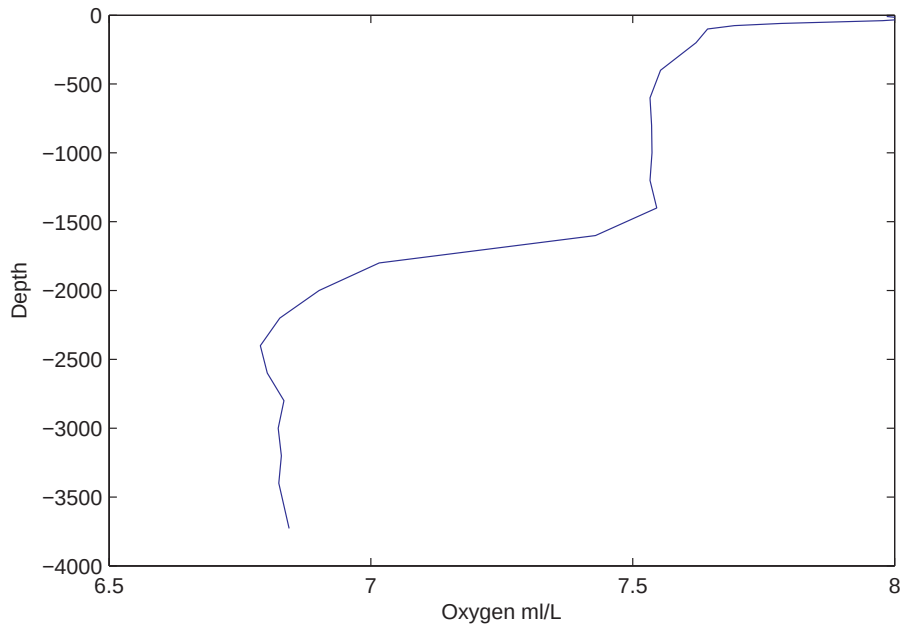

Figure 2.5: An example of a typical oxygen profile in the Greenland Sea measured during June 2007.

To get an idea of the vertical oxygen distribution in the Greenland Sea a station measured in June 2008 is shown in Figure 2.5. The oxygen profile shows a high concentration in the surface layer due to biological production. The intermediate layer

indicates the convection by a honogeneous layer followed by a strong gradient. Right below this gradient an oxygen minimum layer is found followed by a slight increase in oxygen concentration that remains fairly homogenous down to the bottom.

Chapter 3

Data and Instruments

3.1 Presentation of the data

Data used in this thesis are from measurements of oxygen with the addition of temperature and salinity from the cruises listed in Tabel 3.1. With a exception the earlier cruises are from the expeditions of R.V. Johan Hjort (Institute of Marine Research, Norway), while the later cruises are from the Arctic Expeditions (ARK) with R.V. Polarstern (Alfred Wegener Institute, Germany). Most of these cruises took place during the northern summer during the years from 1993 to 2008. The data concidered in this work is restricted to the zonal transect along 75°N, between 10°W and 5°E (Fig. 3.1). This area is of great interest since it intersects the deep

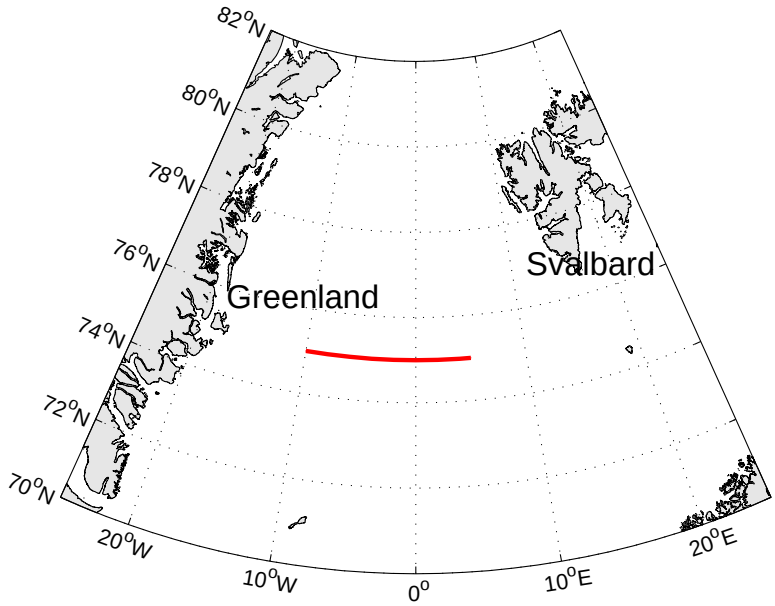

Figure 3.1: Map of the Greenland Sea. Data used are between 10°W and 5°E at 75°N indicated by the red line.

basin of the Greenland Sea and, in addition, it is the area where most data have been collected over the years. In some of the years the presence of submesoscale coherent vortices are seen along the 75°N. Stations measured inside these vortices give

Table 3.1: Information about the data set

Year	Cruise	Date	Latitude	Longitude	Nr. of profiles	Nr. of profiles Averaged 2°W-1°E	Oxygen measurement
1993	Johan Hjort	05.05-07.05	74,87-75,35°N	8,33°W-4,32°E	6	1	Winkler
1994	Johan Hjort	30.05-02.06	75°N	10°W-5°E	5	2	Winkler
1995	Johan Hjort	11.05-14.05	75°N	4°W-3°E	3	1	Winkler
1997	Johan Hjort	18.05-19.05	75°N	4,69°W-4°E	4	1	Winkler
1998	Johan Hjort	17.08-19.08	75°N	8°W-6,96°E	5	2	Winkler
2001	Håkon Mosby	29.06-30.06	74,6-75°N	10,57°W-0,6°E	7	3	Winkler
2003	Polarstern (ARK19-2)	28.04-05.05	75°N	10,58°W-5,48°E	21	4	Winkler, Sensor
2004	Polarstern (ARK20-1)	26.06-30.06	75°N	0,30°W-2,93°E	3	1	Winkler, Sensor
2005	Polarstern (ARK21-1)	31.07-9.08	75°N	9,94°W-2,28°E	9	3	Winkler, Sensor
2007	MS Merian (MSM05/5)	29.07-31.07	75°N	9,32°W-5,50°E	22	4	Winkler, Sensor
2008	Polarstern (ARK23-1)	22.06-28.06	75°N	9,95°W-4,87°E	25	5	Winkler, Sensor

a deeper gradient than the background profiles. In this work it is the background distribution that is of interest, and therefore the stations containing vortices have been removed from the data sets. The extent of the annual data sets vary, with some years only providing a few hydrographic profiles on the 75°N meridian.
Today oxygen can be measured electronically as well as chemically, by the means of an oxygen sensor mounted on the CTD and titration by the Winkler method, respectively. The measurements done by the oxygen sensor give a much more detalied profile than what can be achieved by the Winkler method, since the sensor measures continously while the Winkler method depends on water samples taken at given depths with normally a maximum of 12 or 24 samples on each station. In this work only sensor data taken during the German cruises in 2003-2008 were used (Tabel 3.1).

3.2 Oxygen sensor

The oxygen sensor used by the Alfred-Wegener-Institute is the Sea Bird Electronics 43, SBE 43. This sensor determines dissolved oxygen concentration by measuring the oxygen flux through a polarographic membrane from the sea water to a working electrode, cathode. Oxygen gas molecules are converted to hydroxyl ions (OH-) in a series of reactions at the catode. For each molecule converted the cathode supplies four electrones to complete the reaction. The sensor counts oxygen molecules by measuring the electrones per second (amperes) delivered to the reaction. At the other electrode, the anode, silver chloride is formed and silver ions (Ag+) are dissolved into the solution. The current between the two electrodes gives an output between 0 and 5 volts, which is proportional to the oxygen concentration in the sea water. This voltage measurement is later converted into oxygen concentration. The permeability of the membrane to oxygen is a function of temperature and ambient pressure and is taken into account in the calibration equation used when converting the voltage to oxygen concentration.
Consequently, the chemistry of the sensor electrolyte changes continuously as oxygen is measured, resulting in a slow but continous loss of sensitivity that produces a continual, predictable drift in the sensor calibration with time. This electro-chemical drift is accelerated at high oxygen concentrations and falls to zero when no oxygen is present in the water. Membrane fouling also contributes to the drift by altering the oxygen diffusion rate through the membrane, thus reducing the sensitivity. The oxygen sensor consumes oxygen in the water very near the surface of the sensor membrane. If there is not an adequate flow of new water past the membrane, the sensor will give a reading that is lower than the true oxygen concentration (SBE, 2008a). Accuracy and range for the SBE 43 is shown in Table 3.2.

Table 3.2: Specifications for the Sea Bird Dissolved Oxygen Sensor (from SBE, 2009).

SBE 43 Oxygen Sensor	
Measurement range	120% of surface saturation in all natural waters, fresh and salt
Initial accuracy	2% of saturation
Typical stability	2% per 1000 hours (clean membrane)

3.3 Winkler titration

The method was introduced by Winkler in 1888 and has during the years undergone some modifications to improve its precision (Carpenter, 1965). The oxygen measurements done by Winkler titration requires water samples that are taken from the Niskin bottles mounted around the CTD. The water samples are collected and the reagents needed are added immediatly after the CTD is on deck. This to avoid that the water comes in contact with the atmosphere, which will contaminate the sample by diffusion of oxygen into the water.
The added reagents are manganese chloride ($MnCl_2$), sodium iodide (NaI), and sodium hydroxide (NaOH). After adding the reagents the water sample is shaken thoroughly to make sure the chemicals react with all the dissolved oxygen. A manganous hydroxide percipitate is formed and reacts with the dissolved oxygen in the sample according to the following reactions;

$$Mn^{++} + 2OH^- \rightarrow Mn(OH)_2 \quad \text{(S)}$$

$$2Mn(OH)_2 + O_2 \rightarrow 2MnO(OH)_2 \quad \text{(S)}$$

After this the water samples are stored in the dark untill the percipitation has setteled at the bottom of the flask. Further, sulfuric acid is added to the sample to dissolve the manganese hydroxides. The tetravalent manganese $MnO(OH)_2$ produced act as an oxidation agent and liberates iodine from the iodine ions according to the following reactions;

$$Mn(OH)_2 + 2H^+ \rightarrow Mn^{++} + 2H_2O$$

$$MnO(OH)_2 + 4H^+ + 2I^- \rightarrow Mn^{++} + I_2 + 3H_2O$$

For each oxygen molecule present in the water, one iodine molecule is produced. During titration of the water sample the concentration of iodine is found, and not oxygen directly. The known relation between oxygen and iodine is used to determine the oxygen concentration.
When the acid is added the water sample is placed on a magnetic stirrer and sodium thiosulfate is added to the sample until the endpoint of the titration have been reached. The end point is identified when the solution changes from a yellow or blue

colour to a clear colour. When the titration is done manually starch is added to the water sample, giving the solution a dark blue colour, to make identification of the end point easier. Automatic titration does not require starch since the identification of the end point is done by a photometer.
Measurement of oxygen is a process that requires high accuracy during sampling of the water, storing of the samples, and during the titration. The oxygen is a fluctatious gas and it is therefore crutial that the sampeled water has not been in contact with the atmosphere, and that there are no bubbles in the sample that may cause contamination and errors in the determination of the oxygen concentration. Also it is important to store the sample in a dark and cool place to avoid degradation of the sample. The advantage of Winkler's titration method is that it is accurate and stable. For more detalies on the Winkler method it is refered to Codispoti (1988).

Chapter 4

Correction of the oxygen sensor data

The data from the oxygen sensor must be corrected before they can be used as representative values for the oxygen concentration. The presentation of the work done to correct the sensor data is in the form of single vertical profiles. One of the correction methods has been performed individually on each profile and therefore the individual profil should be presented to show the difference between the methods of correction. Together with the corrected profiles are also the uncorrected sensor profile, the Winkler profile and the bottle data presented to provide all the information that have been used in the correction work. Since 2003 the oxygen concentration has been measured electronically by the use of a SBE sensor. The sensor gives a better resolution in the vertical profiling compared to the Winkler data, since the latter depends on water samples while the former measures continuously. The sensor, however, does not give accurate concentrations and has to be calibrated by the use of Winkler data.

4.1 Calibration of the oxygen sensor data

The advantage of the oxygen sensor is that it gives a more detailed picture of the vertical profiles which is generally not possible to achieve through chemical analyses from water samples due to their limited vertical resoultion. Still, the Winkler data are necessary to correct the sensor data. During the closure of the Niskin bottles the oxygen, temperature, and salinity measured by the CTD is registered and stored in a separate file, called a bottle file. In the following we will call the oxygen taken by the sensor during the downcast for sensor data, the oxygen from the sensor stored in the bottle file for bottle data, and the oxygen measured by the Winkler method for Winkler data. The sensor profile is taken during the downcast, while the bottle and Winkler data are taken during the upcast.
An example of differences between the Winkler data and sensor and bottle data can be seen in Figure 4.1. The dark blue line is the Winkler data, the green line is the sensor data, and the blue dots are the bottle data. There are some differences in the structure of the sensor and Winkler profiles due to the fact that the Winkler profile has few data points. This causes the Winkler profile to be much courser than the

sensor profile, and thereby lose detalies in the structure. From this figure it can be seen that the sensor profile has many more detailes compared to the Winkler profile. Also there are some differences between the different data types, especially between the bottle data and the Winkler data. Since both the bottle and the Winkler data have been measured during the upcast it is assumed that the best method of correction would be to use these two. However, the figure shows that the sensor data have lower concentration compared to the Winkler data while the bottle data have a lower concentration than the sensor data. By using the bottle and the Winkler data to correct the sensor data the difference between the bottle and the sensor data will cause that the corrected sensor data get a to high concentration compared to the Winkler data. Since the bottle data have lower concentration than the sensor data the linear regression between the bottle and the Winkler data will overestimate the difference between the Winkler and sensor data. This can be prevented by using the sensor data in the linear regression with the Winkler data in stead of the bottle data.

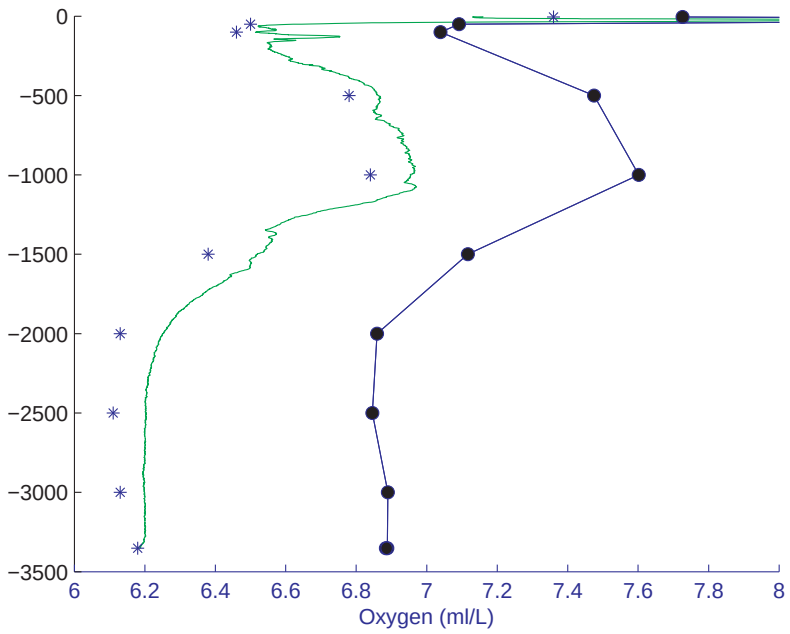

Figure 4.1: The Figure shows the oxygen sensor data profile (green), the bottle data (blue asterix), the Winkler data profile (blue), and the Winkler data points (black).

Because of the possible drift in the sensor with time, as mentioned in section 3.2, one will expect an offset between the sensor measurements and the Winkler mesurements. Ideally the sensor data should only have a shift in value compared to the Winkler data. To see how well the sensor data compare with the Winkler data the difference between the two have been calculated for 2003 and 2007. This difference is calculated by subtracting the sensor data and the bottle data from the Winkler data at the same station and depth for each data point. In the histograms (Figs. 4.2a and 4.2b) the difference between the Winkler data and the sensor and bottle data are shown for all stations at all depths giving drift over depth and time. Time is here shown as measurement numbers where 1 represents difference

for the surface measurement of the first station in consideration, and the following numbers give the difference for each datapoint continuously with depth and station. Thus, giving the difference for each station, as a result of pressure hysteris, and the drift over time in general, possibly as a result of the electro-chemical degradation of the oxygen sensor. For each station there is a pattern giving small differences in the surface values and an increasing difference according to the depth of the measurements/with depth.

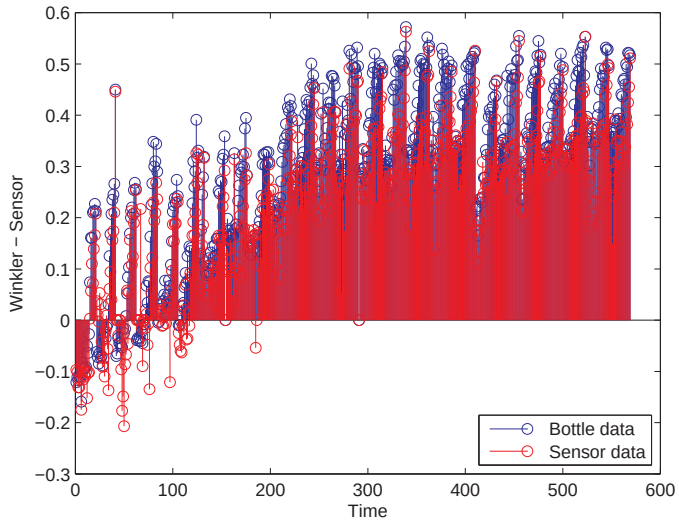

(a)
2003

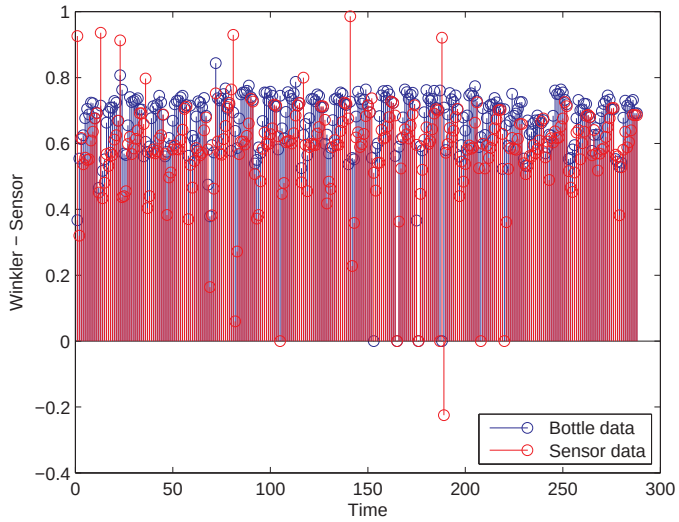

(b)
2007

Figure 4.2: Difference between the sensor, bottle, and Winkler data and drift over time in 2003 and 2007

In 2003 there are significant variations in the drift over time, starting with negative differences in the surface and positive differences in the deep layers of

the first few stations. Further, the difference is positive, however, the difference is varying with depth giving a larger difference at the bottom than at the surface. The mean difference for the all the data is 0.301 ml L^{-1} and 0.236 ml L^{-1} for the bottle and sensor data, respectively. However, since there are large disturbances in the beginning of the time series the mean without the first two hundred data points has been calculated giving a mean value of 0.395 ml L^{-1} and 0.321 ml L^{-1} for the bottle and sensor data, respectively.
In 2007 there are some variations in the drift at the individual stations that probably are due to pressure changes. However, in general there are hardly any changes in the drift over time. In contrast to 2003 the difference in 2007 shows a much smoother pattern, where the differences are mainly of the same magnitude. This can also be seen when comparing the pattern in the figure 4.2b with the mean values of the drift, which is 0.669 ml L^{-1} and 0.584 ml L^{-1} for the bottle and sensor data, respectively. These mean values aligne well with the difference seen in the histogram.
It was assumed that there would be an offset between the sensor measurements and the chemically retrieved measurements making it easy to correct the sensor data by linear regression with the Winkler data. However, this turned out not to be the case due to the changes in the offset with pressure and time (Fig. 4.2a and Fig. 4.2b), making the correcting procedure a much more tedious task.

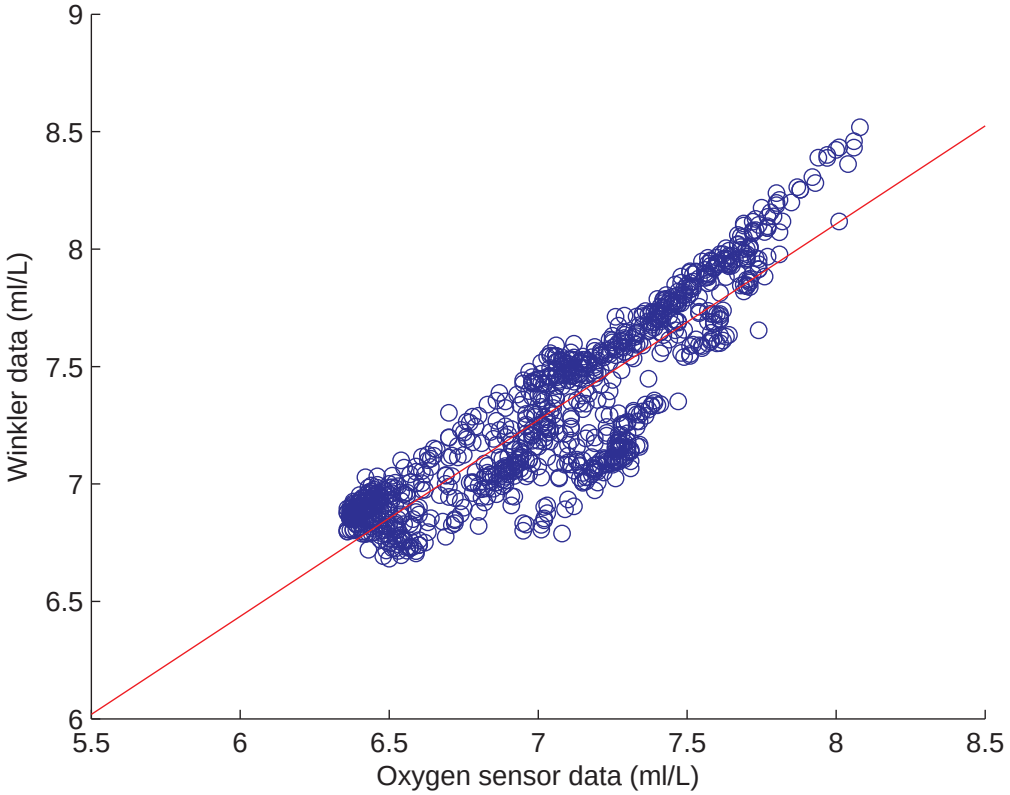

Figure 4.3: Scatter plot of the oxygen sensor data and the Winkler data together with the line of best fit. Data are from 2003.

Several attempts where made in the search for the best method for correcting the sensor data. First a linear regression was done by using all data points from the sensor, bottle, and Winkler data. The data are plotted in a scatter plot with the sensor data given in the x-direction and the Winkler data given in the y-direction (Fig. 4.3). A line of best fit is drawn and the equation for this line is used to correct the sensor data. The equation obtained from the linear regression is of the form;

$$correctedsensor = a + b \times uncorrectedsensor \tag{4.1}$$

This did not give a good match between the corrected sensor data and the Winkler data probably due to the difference in the offset with depth, as well as for the different stations. Further, a linear regression where made by using the data points from the homogenous deep layer. It was assumed that the difference in the homogenous layer would give the best representation of the difference between the sensor and Winkler data. However, this linear regression failed to give a good match between the corrected sensor data and the Winkler data, and were therefore rejected. Because of the difference between the stations the linear regression were now performed on the individual stations to see if this approach would give a better correction. Still, with this approximation the linear regression based on the homogeneous layer did not provide a satisfying match between the corrected sensor data and the Winkler data. Also this correction fail to give a good result for the surface and intermediate layer and has therefore not been further investigated in this thesis.
To deal with the difference in the offset with depth the linear regression where performed on different depth intervals in the further work. The depth was divided into three segments, the upper layer from the surface to 500 meters, the intermediate layer between 500-1500 meters, and the deep layer below 1500 meters. This was done to give a more correct calibration, since the oxygen concentration within these segments vary significantly from each other.
The Figures 4.4a and 4.4b show two selected stations from 2003 and 2007, and some of the correction methods that have been used. The light blue line shows the sensor profile corrected by use of linear regression between the bottle and the Winkler data. The red line shows the correction due to linear regression between the sensor and the Winkler data, and the black line shows the correction due to linear regression between the bottle and the Winkler data done on each station individually.
The tree methods of correction shown here have been divided into the three segments according to depth.
The light blue line in Figures 4.4a and 4.4b shows the sensor profile corrected by the use of the bottle data. In 2003 this gives a bit lower values than the Winkler profile in the upper 500 meters, and a bit higher values for the rest of the profile, except in the near bottom layer beneath 3000 meters. In 2007 the bottle correction shows a close fit to the Winkler profile in the upper 500 meters, and somewhat higher values in the intermediate layer. In the bottom layer this correction shows again a close fit to the Winkler profile.

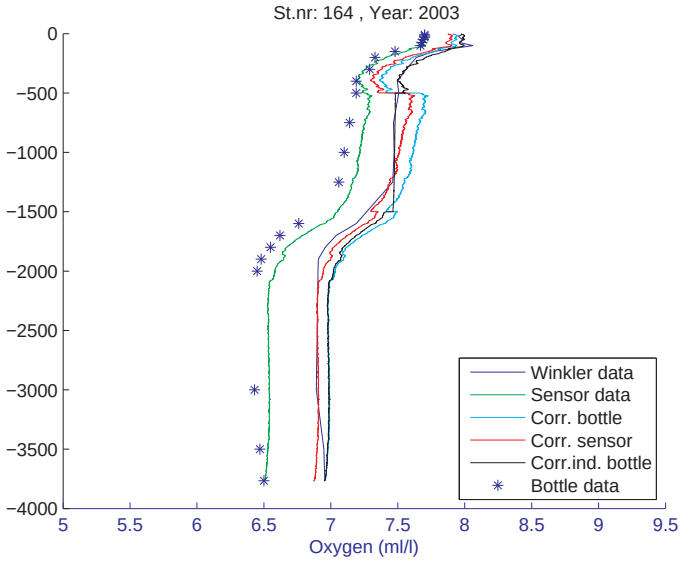

(a)

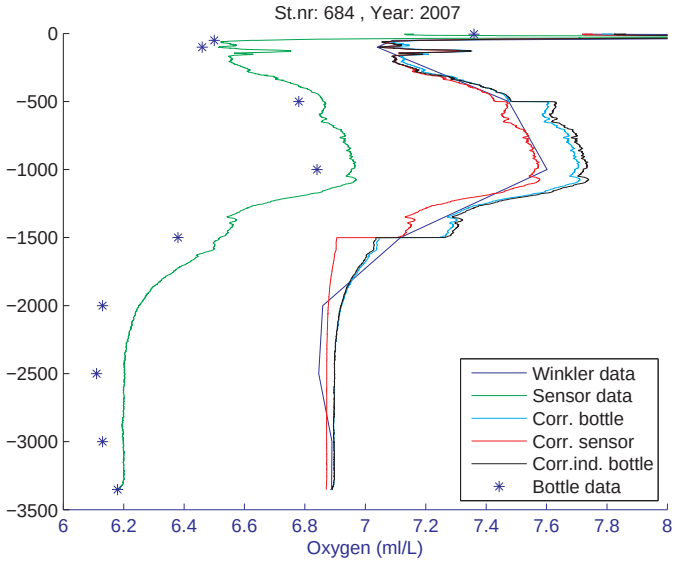

(b)

Figure 4.4: Two selected stations from 2003 and 2007 showing the different correction methods investigated togethet with the uncorrected sensor data, the Winkler data, and the bottle data.

The red profile gives the sensor profile corrected by the use of the sensor data. In 2003 the corrected profile shows lower values than the Winkler profile in the upper 500 meters, a close fit in the intermediate layer, and a bit varying results for the bottom layer. In the first part down to 2000 meters the sensor correction shows somewhat lower values, in the next 600 meters it shows high values, and in the last part it shows low values compared to the Winkler profile. In 2007 the sensor correction shows a close match to the Winkler profile throughout the water column with some minor exceptions, such as at the end of the intermediate layer and at the top of the bottom layer. Here the correction shows slightly lower values compared to the Winkler profile.

The black profile shows the corrected sensor profile by the use of the bottle data on each station individually. In 2003 this method shows a bit high values throughout the whole profile. The difference between the corrected profile and the Winkler profile increases with depth down to 2700 meters depth approximately. Below this depth the difference decreases with depth down to the bottom where it coincides with the Winkler profile. In 2007 the individually corrected profile shows a close match in the upper 500 meters, somewhat higher values in the intermediate layer, and a close match in the bottom layer.
Studying these profiles give that in 2003 the individual correction with bottle data is best for the surface and intermediate layer, while the correction with the sensor data gives the best result for the bottom layer. In 2007 the correction with the sensor profile gives the best result for the whole water column, however, the other two corrections give a better result for the gradient between the intermediate and the deep layer.
These statements are general. There are some differences among the stations, where in some cases other methods give a better result. However, there are not one method that is significantly better than the other methods.

4.2 Summary and discussion

The oxygen sensor has been used lately to simplify the collection of oxygen data since use of the Winkler method is labor intensive and time consuming. The assumption was that the oxygen sensor could be used at all stations while the Winkler method was only used at a few stations as a mean of collecting data for later correction of the sensor data. However, the correction of the sensor data has proved to be more tedious and time consuming than first assumed. The problem is due to the changes in the measuring instrument due mainly to pressure, but also to time degradation in the instrument. In 2003 the difference between the sensor and the Winkler data variate more than in 2007, however, the value of difference is somewhat larger in 2007. Large variations in the difference between the two data sets make the correction procedure more tedious than a more consistent difference.
In this work the correction was done by linear regression between the sensor and the Winkler data, and the bottle and the Winkler data. It is assumed that using the bottle data as means of correction is more accurate due to the fact that the bottle data is taken during the upcast together with the Winkler data, while the sensor data is taken during the downcast. The reason for this assumption is due to the drift of the ship causing the location of the down- and upcast to be slightly different. By comparing the difference between the Winkler data and the other two data set this shows that there is a larger difference between the Winkler and the bottle data than the Winkler and sensor data.
The correction was first conducted by only using the data from the most homogenous bottom layer in the linear regression, however, this gave a poor correction to large parts of the profile except in the bottom layer. Based on this discovery a second correction was conducted then dividing the data into three depth segments according to the upper layer, the intermediate layer and the bottom layer. Sepa-

rating the data into intervals and running separate linear regressions gave a much improved correction of the profile. The disadvantage of this method is visible at the gradient at intermediate depth where the corrected profile shows a structure distorting significantly from the Winkler profile suggesting that the gradient should be corrected separatly as well.
When the upcast and downcast do not match the sensor profile should be corrected by using the downcast data. To correct for the pressure hysterisis it is probably necessary to make the adequat changes in the program converting the measured voltage into oxygen concentration.

Chapter 5

Results

Previously there have been made many investigations of the convection and deep water formation in the Greenland Sea. In the recent years a major change has been discovered revealing that the convection has reduced in vertical extent possibly leading to the increase in temperature and salinity over the 1990s and 2000s. The convective events and bottom water changes from 1993 to 2008 will be investigated in the following. The main parameter used is the oxygen concentration, however, the temperature and salinity are also included to get a better indication of which water masses are present.

5.1 Zonally vertical sections

In order to get a good overview of the annual situations and possible changes along the 75°N in the Greenland Sea the distribution of temperature, salinity, and oxygen across the Greenland Sea is presented in Fig. 5.1, 5.2, 5.3, 5.4, 5.5, and 5.6. The temperature and the salinity are from the bottle files, and the oxygen is measured by Winkler titration. The Winkler data are used since they give the most reliable data and are available for the years in question (Tabel 3.1). The vertical sections show only the distribution below 500 meters depth. The upper 500 meters are not concidered here since it is subjected to seasonal changes which is not of interest in this context.
By plotting the vertical profiles in contoure plots gives a snapshot of the distribution at that particular time and area. Since the hortisontal distance is much larger than the vertical distance in the profiles it is necessary to exaggerate the vertical distance in the plots to be able to show the patterns of distribution. Ocean Data View (ODV) is the program that has been used to present the vertical sections (Schlitzer, 2004). This program sorts and displays the data according to station number and coordinates, giving zonal sections if requested. In the ODV-sections the display of the data can be manipulated to some extent by expanding the colourgrid thereby influencing, to some degree, the distrubtion of the section. If there are few data points available the display will be less accurate due to the lack of data and the following manipulation of the colourgrid to make usefull section plots. The data points are shown as black dots to show the horizontal and vertical distance thereby giving the degree of the manipulation of the colourgrid.

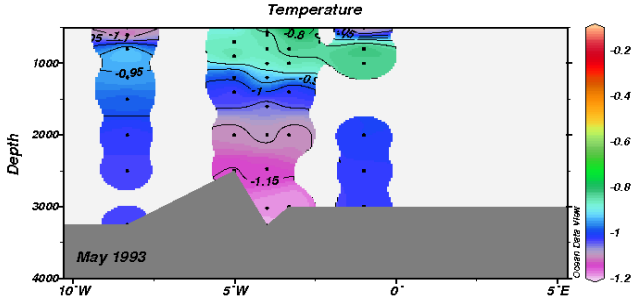

(a)

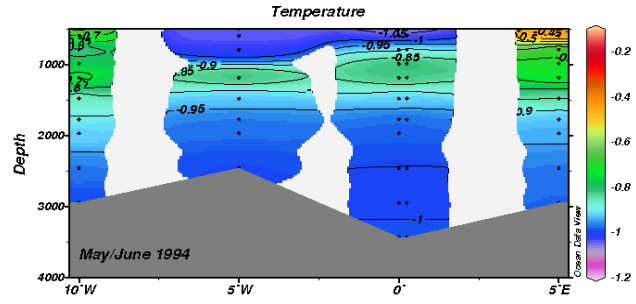

(b)

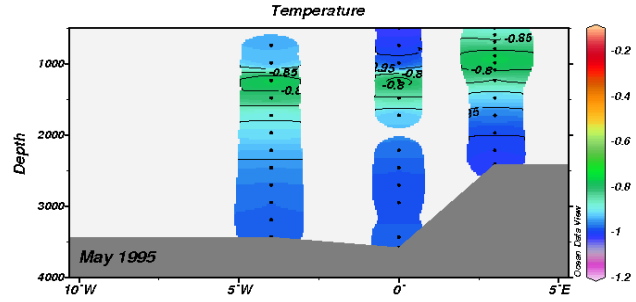

(c)

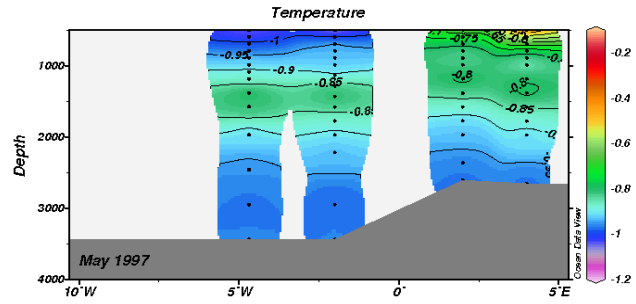

(d)

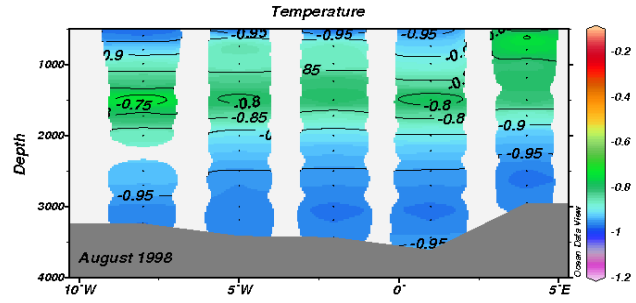

(e)

Figure 5.1: Zonal section showing the temperature for the different years

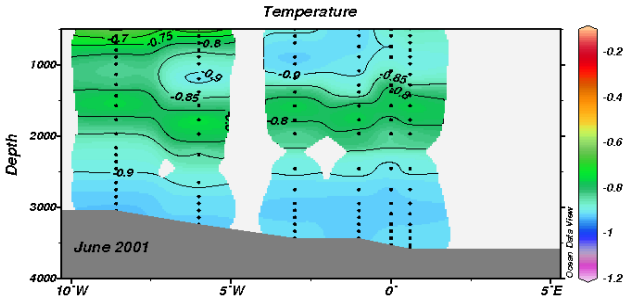

(a)

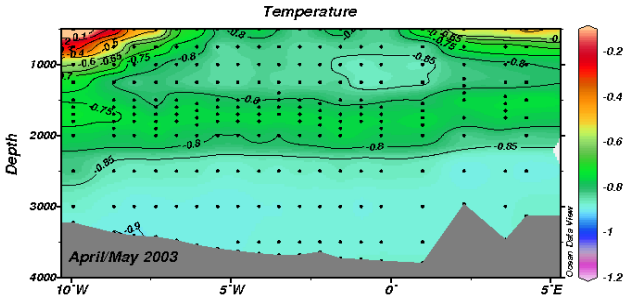

(b)

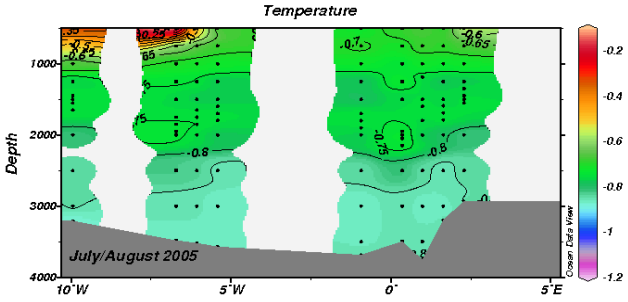

(c)

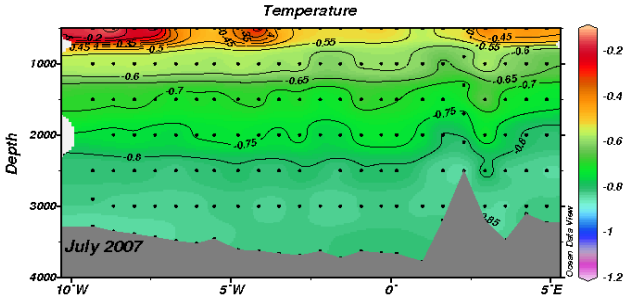

(d)

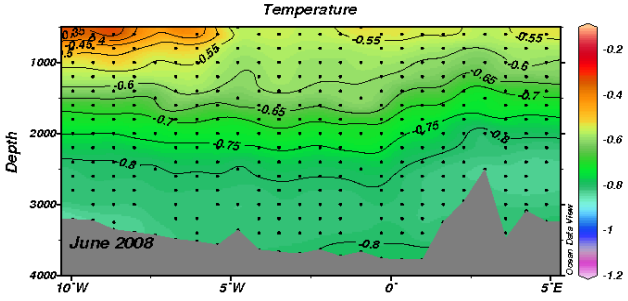

(e)

Figure 5.2: continued: Zonal section showing the temperature for the different years

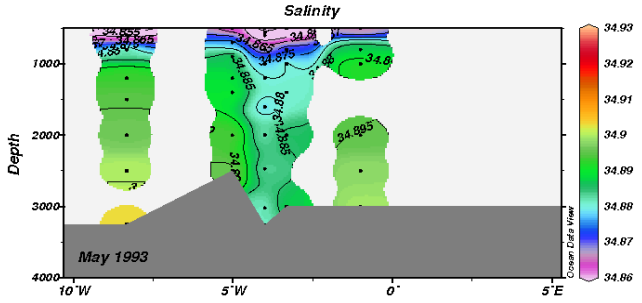

(a)

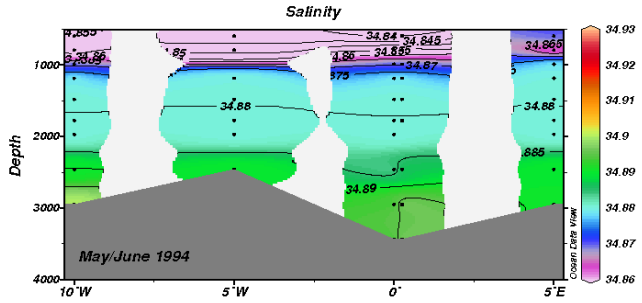

(b)

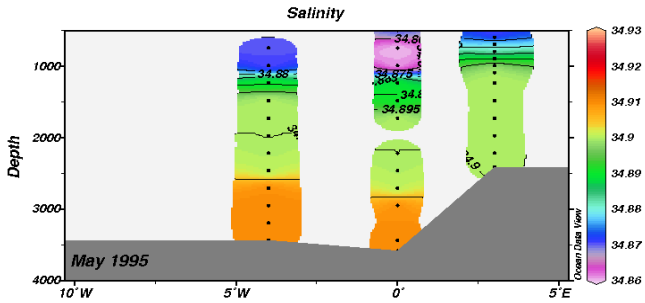

(c)

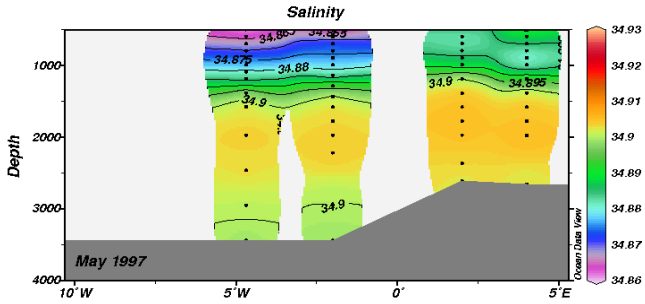

(d)

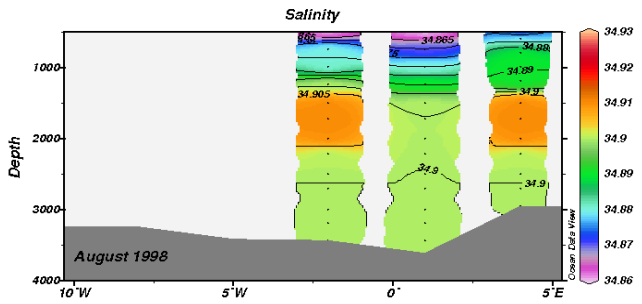

(e)

Figure 5.3: Zonal section showing the salinity for the different years

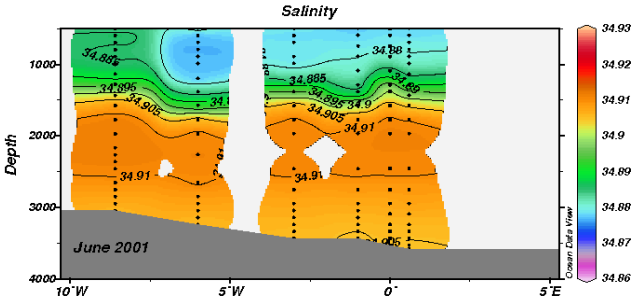

(a)

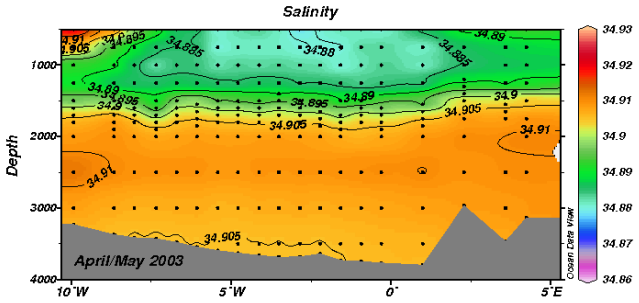

(b)

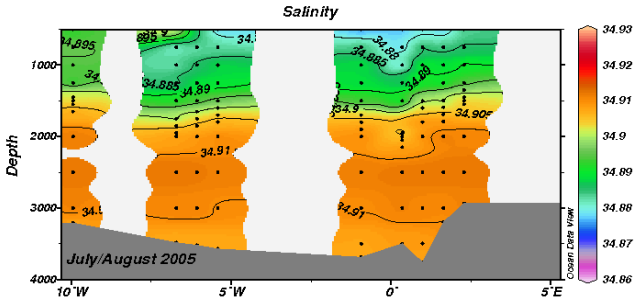

(c)

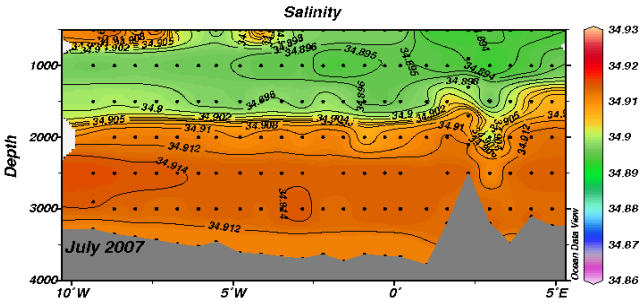

(d)

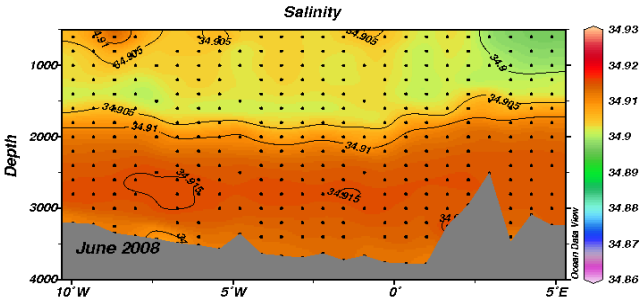

(e)

Figure 5.4: cont.: Zonal section showing the salinity for the different years

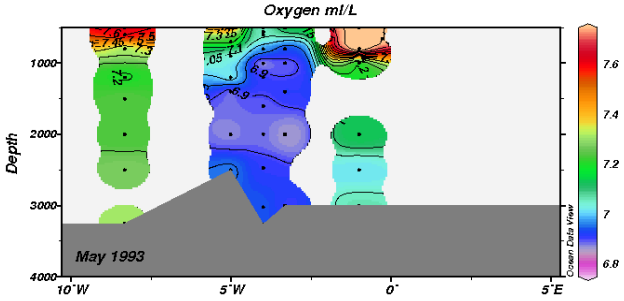

(a)

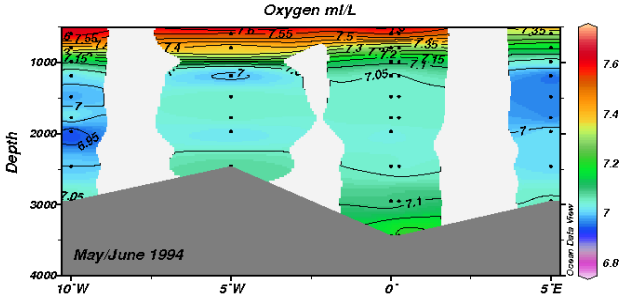

(b)

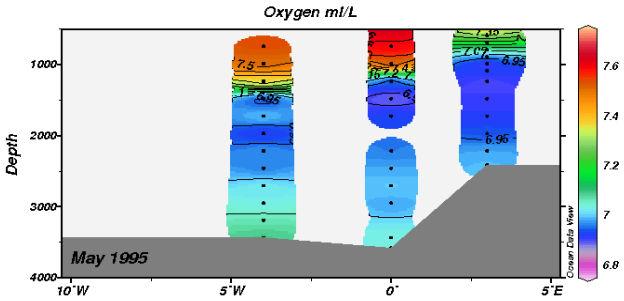

(c)

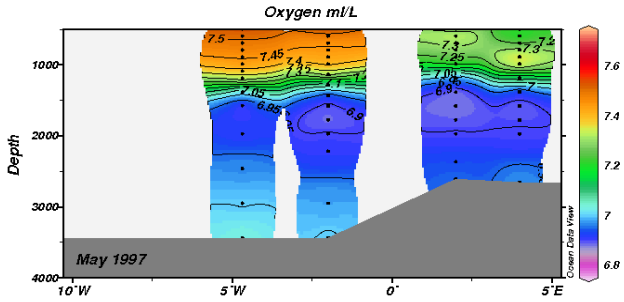

(d)

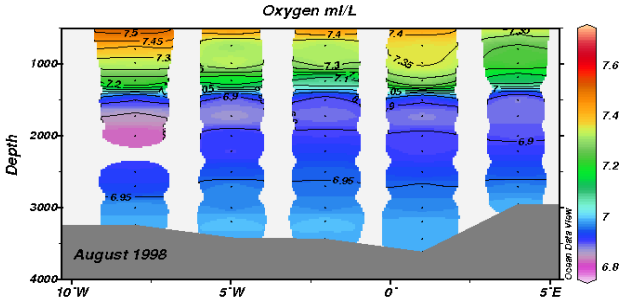

(e)

Figure 5.5: Zonal section showing the oxygen concentration for the different years

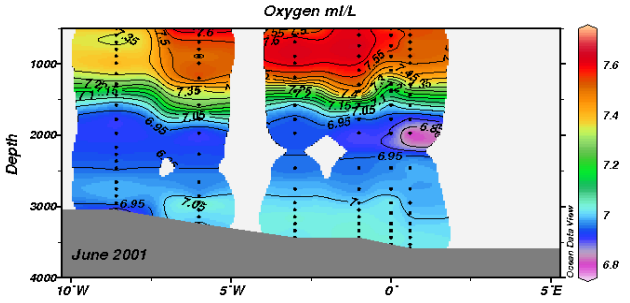

(a)

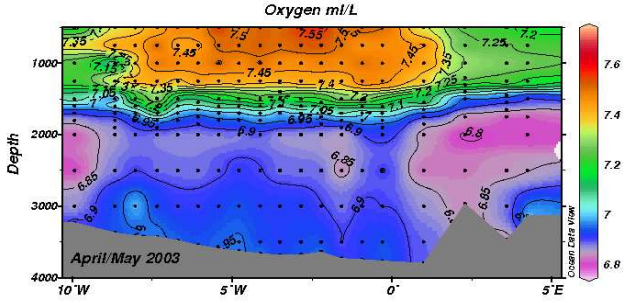

(b)

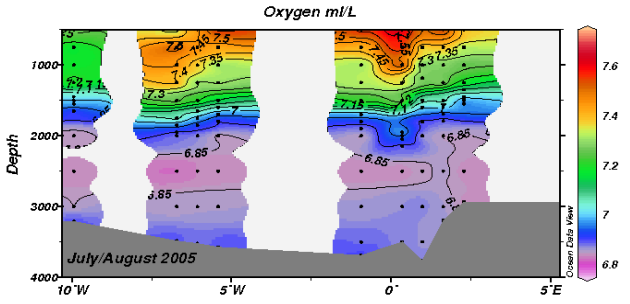

(c)

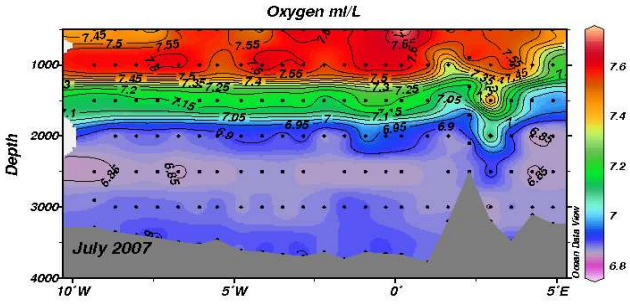

(d)

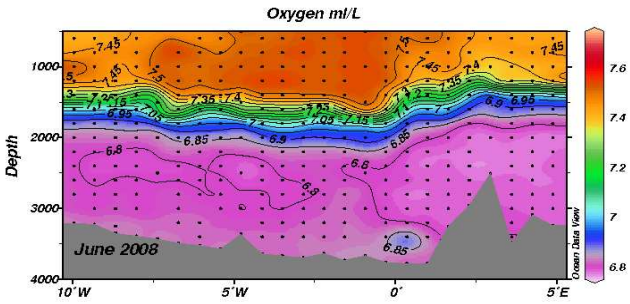

(e)

Figure 5.6: cont.: Zonal section showing the oxygen conc. for the different years

In these sections the same expansion of the colourgrid has been used which is the reason for the white areas in some of the sections with few data points. The zonally vertical sections for each year available will be described in the following.

5.1.1 Temperature

The most dominant feature seen in the temperature sections (Figs. 5.1 and 5.2) is an increase in temperature over the whole water column during the years and the separation of the water column by a temperature maximum, T_{max} during most of the years. In 1993 the T_{max} is located at 700-800 meters and has typically a temperature above -0.85°C. This T_{max} is easy to recognise in the following years. The depth of this layer descends reaching close to 2000 meters in the early 2000s along with an increase in the T_{max} value to above -0.75°C in 2005. From 2007 the T_{max} layer is no longer present in the Greenland Sea. Instead the temperature is decreasing continously with depth as seen in 2007 and 2008 (Fig.5.2d and Fig.5.2e). The general vertical distribution shows that the temperature decreases away from the T_{max} in both the layer above and below this T_{max}. The temperature is slightly lower in the deep layer below the T_{max} compared to the upper layer. The temperature shows an increasing trend over this time series both above and below the T_{max}, see Tabel 5.1. The upper layer is quite cold during the 1990s, but from 2001 a clear increase in temperature can be seen during the following years. From 2003 an inflow of warmer water is clearly seen on both sides, where the strongest signal is seen on the western side. Over the following years this signal advects/mixes across the section. In the layer below the T_{max} very cold water is seen in 1993 in the deeper parts near 5°W, with temperatures below -1.15°C. An increase in temperature is seen in the bottom layer during the years to slightly below -0.8°C in 2008.

5.1.2 Salinity

The most dominating feature seen in the salinity sections (Figs. 5.3 and 5.4) is the increase in salinity in the whole water column during the years and the gradient at intermediate depth separating the highly saline deep water from the less saline upper water. In general the salinity gradient is located close to the T_{max}, at 700-800 m in 1993 and descends to about to 2000 m in 2005. In 2007 and 2008 the gradient is still located at 2000 m depth, however, it is significantly weaker. The gradient is significantly weaker in 2008 compared to 2007.
The general vertical distribution shows that the salinity increases with depth, but there are only small differences in the value range, with most variation in the upper layer above the gradient. Below the gradient there are few horizontal variations, and the layer is nearly homogeneous. The salinity shows an increasing trend over the years along with a homogenisation of the whole water column (see Tabel 5.1). The upper layer remains quite fresh in the 1990s, but from 2001 and onwards an increase in salinity can be seen. During the years there is an increase in salinity from 34.89 in 1993 to 34.915 in 2008.

Table 5.1: Values from the different parameters investigated sorted according to the vertical structure in the zonal sections

Year	T_{max}	T^{above}	T^{below}	S^{grad}	S^{above}	S^{below}	$O_2{}^{grad}$	$O_2{}^{above}$	$O_2{}^{below}$
1993	-0.74- -0.87	-1.13- -0.74	-1.20- -0.94	34.87	34.85-34.86	34.88-34.90	7.20-7.30	7.52-7.86	6.84-7.31
1994	-0.79- -0.73	-1.07- -0.61	-1.08- -0.87	34.85-34.86	34.83-34.87	34.88-34.90	7.10-7.20	7.28-7.70	6.92-7.30
1995	-0.78- -0.76	-1.00- -0.85	-1.00- -0.90	34.88-34.87	34.86-34.88	34.90-34.91	6.90-7.10	7.19-7.63	6.88-7.00
1997	-0.88	-1.08- -0.88	-0.98- -0.88	34.89	34.86-34.89	34.90-34.91	6.90-7.10	7.19-7.61	6.87-7.04
1998	-0.85- -0.78	-0.97- -0.85	-0.97- -0.85	34.89	34.86-34.88	34.90-34.91	6.90-7.10	7.12-7.55	6.81-6.98
2001	-0.80- -0.74	-0.92- -0.84	-0.92- -0.84	34.89	34.88-34.89	34.90-34.91	6.90-7.10	7.20-7.63	6.76-6.93
2003	-0.80- -0.75	-0.88- -0.74	-0.91- -0.85	34.89	34.88-34.89	34.90-34.91	6.90-7.10	7.20-7.58	6.79-7.04
2005	-0.76- -0.74	-0.79- -0.13	-0.88- -0.78	34.89	34.88-34.90	34.90-34.91	6.90-7.10	7.17-7.65	6.82-6.98
2007	-0.74- -0.62	-0.62- -0.09	-0.86- -0.80	34.90	34.89-34.90	34.90-34.92	6.90-7.10	7.47-7.79	6.84-6.91
2008	-0.70- -0.65	-0.63- -0.24	-0.84- -0.70	34.90	34.90	34.91	7.10-7.55	7.28-7.57	6.76-6.83

5.1.3 Oxygen

The most dominant feature seen in the oxygen sections (Figs. 5.5 and 5.6) is the decrease in oxygen concentration over the years in the deep layer and the increase in the vertical extent of the upper layer. The oxygen concentration gradient follows to a large extent the location of the T_{max} and the salinity gradient. In 1993 the oxygen gradient is located at 800 m and descends to approximately 1700 m in 2008. The general vertical distribution shows that the highest concentration is in the upper layer above the gradient, while the lowest concentration can be found in the deep layer. The oxygen concentration in the upper layer varies over the years investigated giving some years with increased concentration and some years with a decreased concentration when comparing succesive years. The concentration is somewhat higher close to the central Greenland Sea at approximately 5°W to 0°W for some years. In the layer below the gradient the oxygen concentration is quite high in the early 1990s, with a concentration above 7.2 ml L^{-1}. From 1997 there is a slow decrease in the concentration over the following years and from 2003 the decrease in concentration accelerates reaching below 6.85 ml L^{-1} in 2008 in the whole deep layer. An oxygen minima can be found in a layer right below the gradient for most of the years and is more prominent on the sides for some years. This minima can clearly be seen from 1998 and in the following years as the areas with concentration below 6.85 ml L^{-1}. An overall trend for the whole time series shows that there has been a decrease in the concentration in the deep layer, see Tabel 5.1, and that the vertical extent of deep layer has become smaller over the years.
From the zonal sections it can also be seen that the highest oxygen concentration can in general be found in the central part of the Greenland Sea and particullary between 6°W and 1°E. Based on this it is assumed that this is an area influenced more severly by convective events than the rest of the section and the central part between 2°W and 1°E have been investigated separatly in the following sections.

5.2 Changes in the central part of the Greenland Sea

Hov-Möller diagrams present a good opportunity to view data from several years in one figure making it easier to see changes and trends. In this part of the work the central Greenland Sea is the area of interest because this area is thought to be a main area for convection. To get an overview of the general changes in this area the data from stations between 2°W and 1°E have been averaged over the same depths for each year giving one annual profile for the whole area. The collection of data has not been consequent for every year and therefore the data have been measured at different longitudinal coordiantes during the different cruises. Thus there will be a varying amount of data between the years.

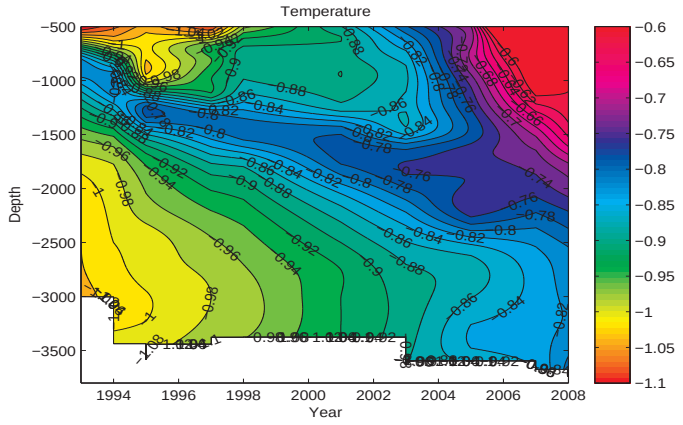

(a)

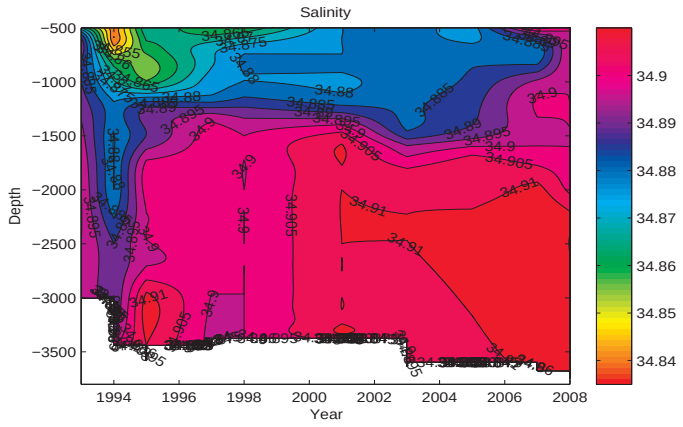

(b)

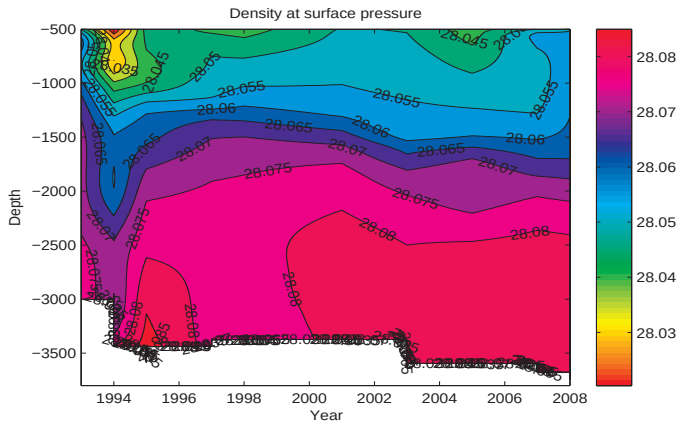

(c)

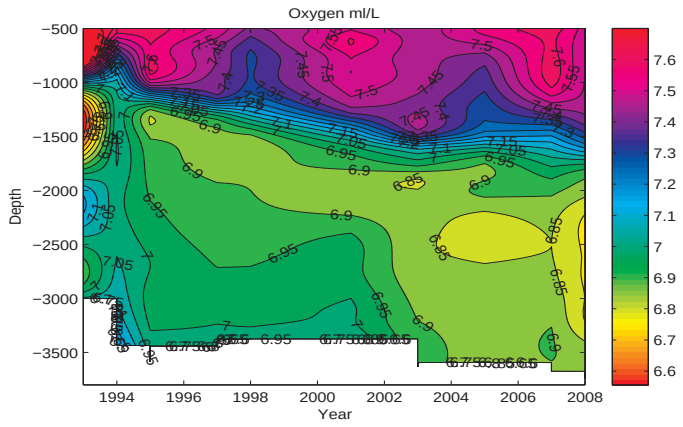

(d)

Figure 5.7: Temperature, salinity, density, and oxygen concentration averaged from 2°W to 1°E.

Since the Winkler data have a very limited vertical resolution a spline interpolation was conducted on the average profiles to give values for each meter in depth. The spline interpolation method use the data set together with a give vector giving the wanted depth to fill out the data set with estimated values. The result is a vector of values consisting of the Winkler data and estimated oxygen values for the depths missing values, thereby providing a profile with oxygen values for each meter for the whole vertical profile. The spline interpolation is done to each profile individually giving an approximation to how the profile would look like with more data points, using the existing data points. The structure of the profiles undergo minor changes due to the spline interpolation, however, the small structures that are not seen from the existing datapoints may be incorrect. There are possibilities that errors may occure due to this, however, the small scale structure is not of great concern here. The same has been done for the temperaure and salinity. The averaged profiles are then plotted continually in a contour plott over the years in question.
The distribution of the temperature shows that the water column is divided by a temperature maximum, T_{max}, for most of the years and that the temperature in general shows a gradually increasing trend as well as the distribution becomes more homogenous. In 1993 the T_{max} is located at about 800 meters depth, dividing the water column into two layers of cold water above and below the T_{max}. During the next years the T_{max} is descending to 1700 meters in 2005. In 1998 the T_{max} layer has expanded vertically into a broader band at intermediate depth, extending from 1100 to 1600 meters. The lower limit of the broad T_{max} has a rapid descend over the next years, while the upper limit is descending more slowly at first, until a more rapid descend in 2001. In 2005 the T_{max} has a very weak upper limit, and in 2007 the T_{max} disappeared completely.
An increase in temperature of the water column happens both above and below the T_{max}. In the last four years from 2004 the temperature increase of the column is more progressive. This progressive increase in temperature is more visible in the upper layer than in the lower layer, where the temperature increase is more continous over the whole timeperiod. After the T_{max} disappears there is a monotonical decrease in temperature with depth. The temperature above and below the T_{max} was the same in the beginnig of the periode, both showing a temperature of -1.08°C. The increase in temperature was stronger in the upper layer reaching a value of -0.62°C in 2008, while in the bottom layer it only increased to -0.8°C.
From figure 5.7b the main feature in the salinity changes are the homogenization of the deep layer below the gradient with time. The gradient in salinity is located at quite shallow depth in 1993, where it is found at about 500 m depth. During the years it gradually descends to about 1500 m with the exception of 1994 where the whole water column have low salinity. In the last two years, 2007 and 2008, the gradient is very weak, separating water with a salinity value of 34.895 from water with salinity 34.910, giving a nearly homogeneous water column. In both the upper and deep layer there is an increase in salinity over the years with the exception of 1994. The upper layer have a slightly lower salinity than the deep layer, but the difference between the layers becomes less after the disapperance of the T_{max}.
The main feature seen in the density distribution (Fig.5.7c) is the gradient at intermediate depth and the increase in density in the deep layer from 2000. The gradient

shows a slowly descending trend from 800 m in 1993 to 1500 m in 2008 with the exception of 1994. In the upper layer the density is fairly the same for most years. In the layer below the gradient there are minor changes during the years, with the exeption of 1994 where the water has somewhat lower density than most years. During the 1990s the density experiences some changes while in the 2000s the density distribution is approximately the same for all years.
Figure 5.7d shows the changes in the oxygen concentration throughout the water column. The depth of the gradient separating the upper and deep layer shows a descending trend. The descend is most rapid during the first part of the period and reaches about 1700 meters depth in 2008. The oxygen concentration in the gradient mainly separates the water column in two where the values change from 6.95 ml L^{-1} to 7.00 ml L^{-1}.
In the upper layer there are no particular trend, but there are some fields of high concentration with varying vertical and timely extent. The years with highest oxygen concentrations are 1993, 1995, 2001 and 2007. The vertical extent of the high oxygen concentration starts in 1993 and reaches down to 800 meters. In 1995 it reaches down to 1000 meters, in 2001 down to 1400 meters, while in 2007 it extends down to 1000 meters. In 1998 there is low oxygen concentration in the upper layer compared to the rest of the timeseries. The oxygen value range is from 7.00 to 7.60 ml L^{-1}.
Below the gradient the oxygen value range is from 6.60 to 6.95 ml L^{-1}. There is a decreasing trend in oxygen in the deep layer starting with values slightly above 7.0 ml L^{-1} to below 6.8 ml L^{-1}. An oxygen minimum with values below 6.9 ml L^{-1} is seen right below the gradient from 1995. At the end of the period, from 2003, the oxygen minimum field becomes broader reaching from the gradient nearly to the bottom.

5.3 Convection depth

The distribution of oxygen concentration in the water column can be used to identify the convection depth. The more or less homogeneous column found below the surface layer are the remnants of the last winter convection. The convection depth is said to be the same depth as where the homogeneous column ends and the gradient between the ventilated and the deep layer is located.
When investigating the data to find the convection depth the uncorrected sensor data can be used. Even though the concentration value is incorrect, the structure of the profile can give the convection depth. For the years lacking sensor data, Winkler data have to be used to identify the convection depth. The Winkler data give a coarser profile, due to the limited number of data points, and therefore give a less exact position of the convection depth. This can be seen in Figure 5.8 where a profile from the oxygen sensor is plotted together with the Winkler profile to compare the vertical structures they provide. This figure shows that the sensor profile is more detalied and give a better view of the vertical structure of the oxygen concentration.
If the mentioned method of identifying the convection depth is applied directly the Winkler profile it shows that the convection depth is located close to 1600 m, but since there is no Winkler data between 1600 and 1750 m there is a possibility

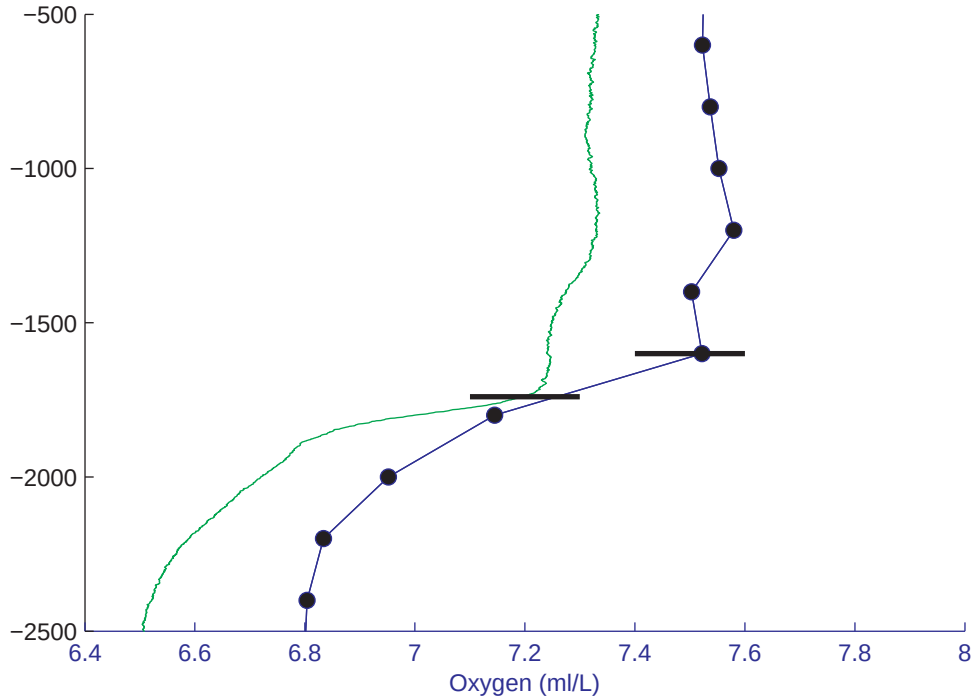

Figure 5.8: The oxygen sensor data profile (green) compared to the Winkler data profile (blue). The black horizontal lines indicate assumed convection depth. Data from 2008.

that the convection depth lies somewhere between those two depths. The sensor profile clearly shows that the convection depth is actually located close to 1700 m. Therefore the use of Winkler profiles may give to shallow convection depths.

In Figure 5.9 the oxygen sensor profiles from the whole section in 2008 are shown. Here it can be clearly seen that the convection depth varies horizontally over the transect with a convection depth of 1100 m at the rim of the basin and a depth of 1700 m in the central parts.

To find the mean convection depth at 75°N the convection depth for each station is identified and an average value for each year is caluculated. The average convection depth from the Winkler data and from the sensor data are shown in figure 5.10 and figure 5.11, respectively. The average convection depth is plotted together with the maximum and minimum interval to give the horizontally variation for each year to provide the whole story of the convective event. The annual vertical profiles used to calculate the average convection depths are shown in Appendix 1.

Figure 5.10 show a descending trend of the convection depth in the 1990s from 600 m in 1993 down to 1200 m in 1997 and 1998. In the 2000s the winter convection reach the same depth at 1200 m for most of the years, except in 2007 where the convection depth only reach 1000 m depth. The maximum depth reaches significantly deeper down the water column for most of the years indicating that there are stations with deeper reaching convective events. Comparing this with the section plots it can be seen that the deeper reaching stations are often located in the central parts of the Greenland Sea.

For the years with sensor data (Fig. 5.11) the same trend can be seen. However, the

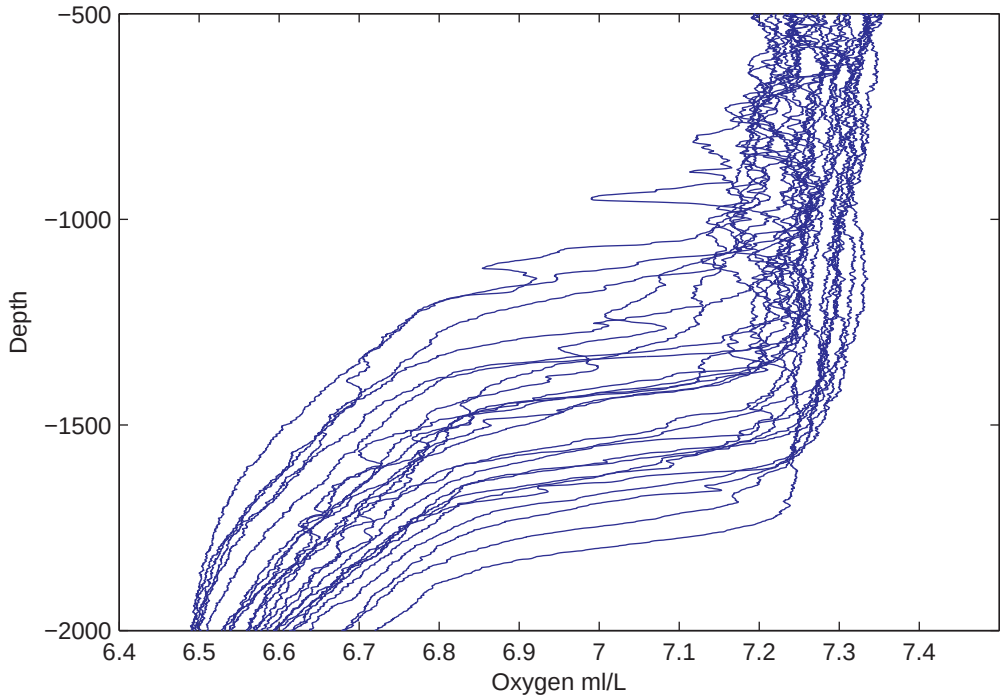

Figure 5.9: The oxygen sensor data give more detalied profiles compared to Winkler profiles. Data from 2008.

sensor shows that the convection depth is somewhat deeper than what is found from the Winkler data. In Figure 5.11 the average convection depth is located below 1400 m for most years except 2007 where it is located at 1100 m depth. The maximum depth also reaches greater depths than what can be seen from the Winkler data.
Further, by comparing the oxygen concentration between two successive years it may be possible to identify the type of convection that took place during the winter. This may provide a fuller picture of the convective events during the winter. It is of interest to see if the oxygen concentration has increased or decreased compared to the year before. In Figure 5.12 profiles from two successive years are plotted together in different colours to easier show any changes in the oxygen concentration. The available successive years are 1993/1994, 1994/1995, 1997/1998, and 2007/2008. Since the convection in this time period has not reached beyond the intermediate layere, the profile figures have a vertical limit from 500 meters depth, which is the depth of the surface layer, to 2000 meters depth giving only the depth interval needed to identify convection depth.
The oxygen concentration in 1993 shows a wider range compared to 1994 (Fig. 5.12a). Two profiles in 1993 differs from the other profiles giving a high oxygen concentration at 700-800 meters depth. Looking apart from these two profiles the oxygen concentration in 1994 is slightly higher than in 1993 above 900 meters depth. In 1995 the oxygen concentration in the intermediate layer is significantly higher than in 1994, reaching down to 1200 and 1400 meters (Fig. 5.12b). Beneath this depth the oxygen concentration in 1994 is in the lower range of the oxygen concentration seen in 1993. In Figure 5.12c the oxygen concentration is similar in both years, but from 1200 m and down to 1500 m the oxygen concentration is slighlty higher in 1998.

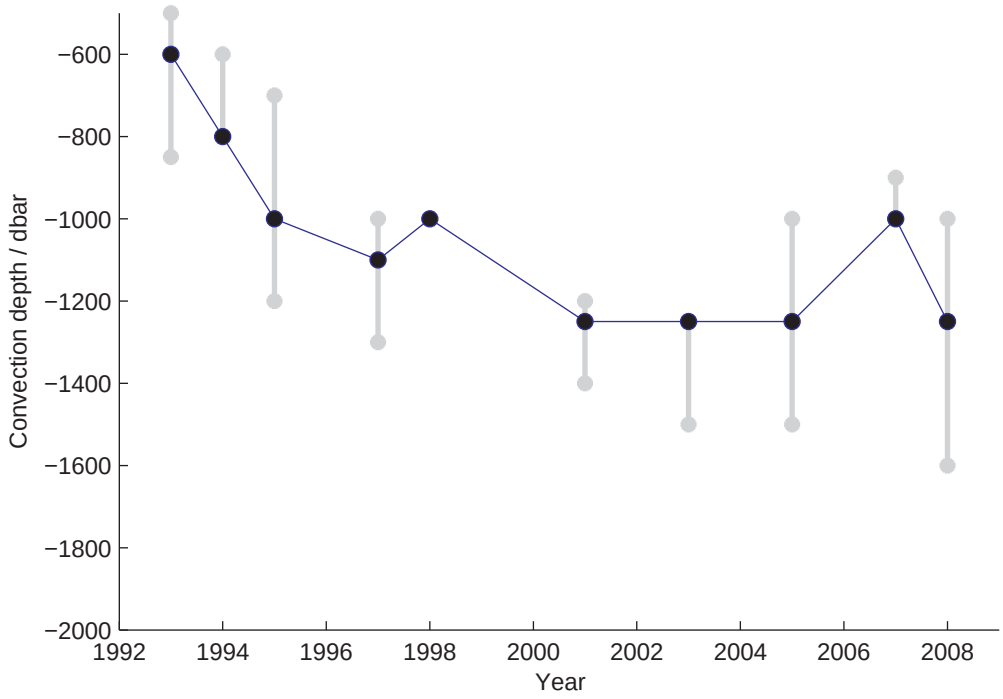

Figure 5.10: The average convection depth (blue line) from the Winkler data for all years investigated with the maximum and minimum convection depth indicated by the grey line.

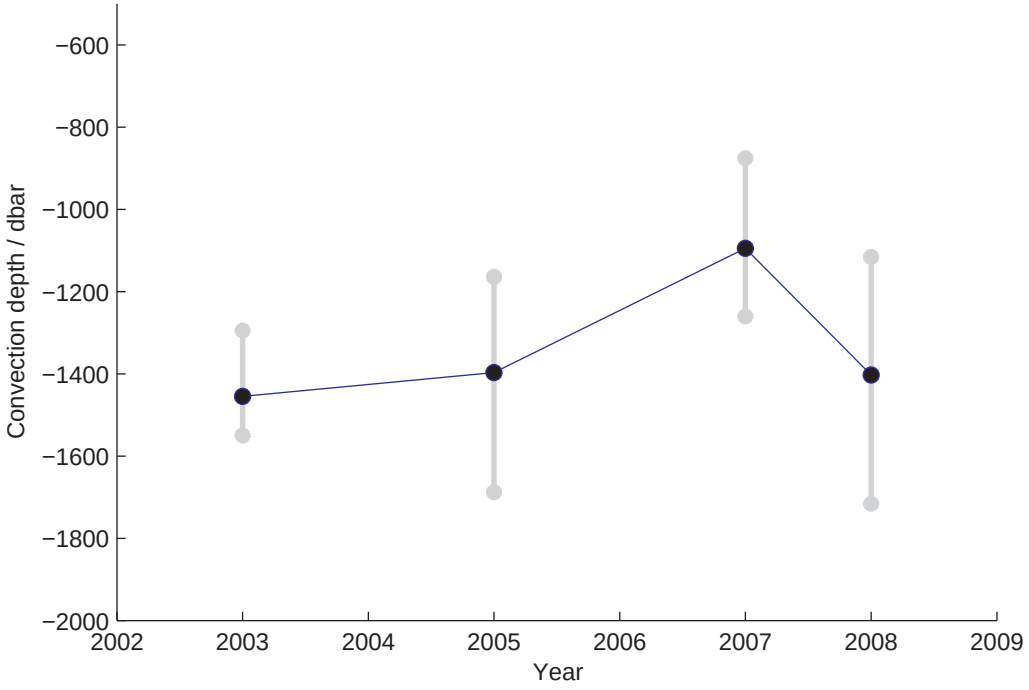

Figure 5.11: The average convection depth (blue line) retrived from the sensor data with the maximum and minimum depths indicated by the grey line.

Figure 5.12d shows that the layer with high oxygen concentration in 2008 penetrates deeper down the water column compared to 2007. However, the concentration has decreased between the two years. In 2008 the layer with high oxygen concentration reaches down to 1600 m depth while in 2007 it only reaches 1100 m depth.

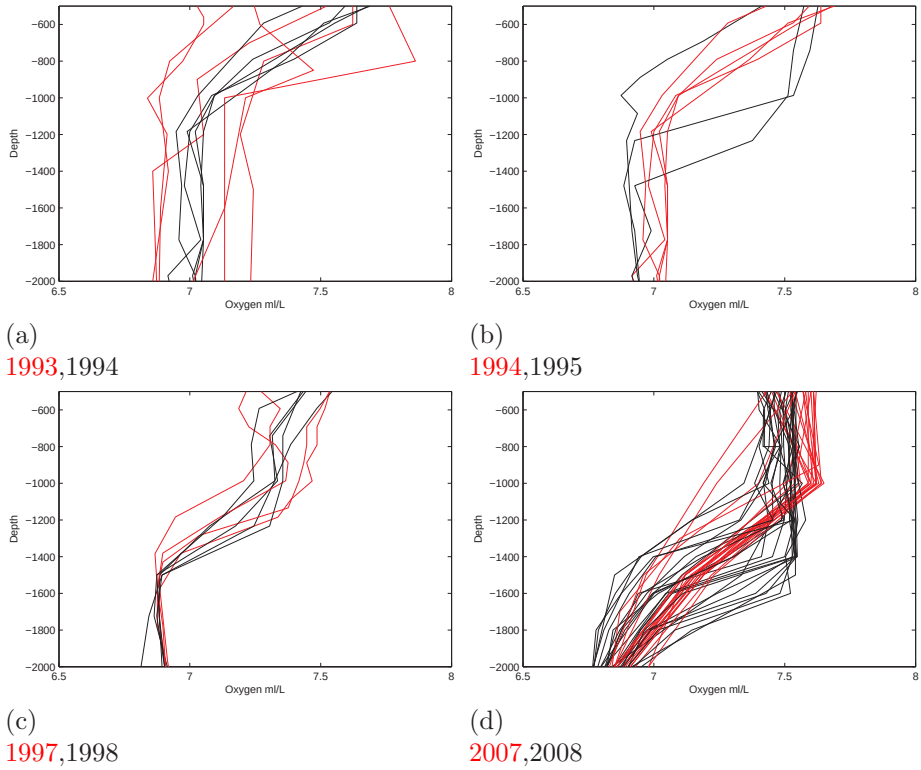

(a)
1993,1994

(b)
1994,1995

(c)
1997,1998

(d)
2007,2008

Figure 5.12: Vertical profiles of oxygen concentration from two succesive years.

5.4 Changes in the deep layers

Another part of this work was to look at the evolution of the oxygen concentration in the bottom layer of the central Greenland Sea. As already seen in the Hov-Möller diagrams the bottom layer has experienced a slight decrease in oxygen concentration over the years in question. Here four depths have been selected and a time series have been made to give a more detalied view of the changes. The selected depths are 2000 m, 2500 m, 3000 m, and 3500 m. The same has also been done for temperature, salinity, and density (Fig.5.13).
In figure 5.13a it can be seen that the temperature has increased in all the lower layers over the years in question. In the first years of the time series all of the four layers are have nearly the same temperature, with only slight differences, but from 1997 the uppermost layer increase at a more rapid pace. The warmest water is found in the uppermost layer during most years with the exception of the early 1990s. The lowest temperature can be found in the 3000 m layer from 1993 to 2005, but from 2007 the deepest layer has the lowest temperatures. The three deepest layers are

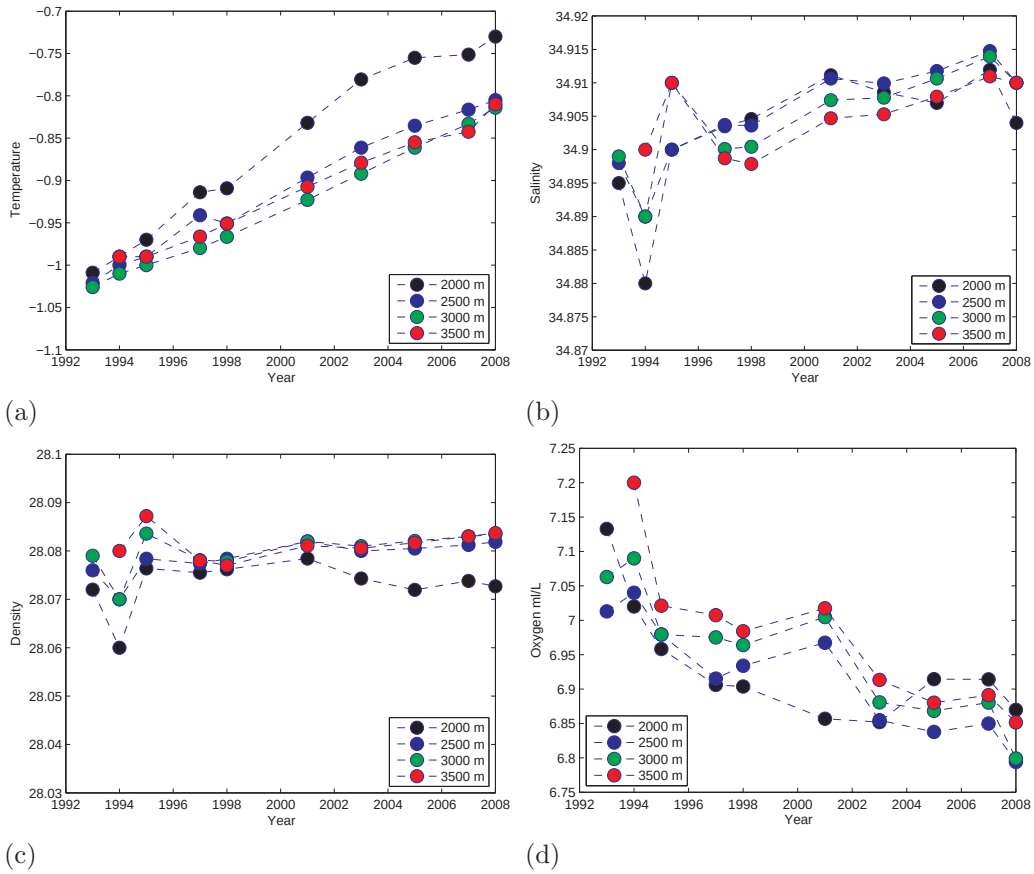

Figure 5.13: Temperature, salinity, density, and oxygen concentration averaged over the central Greenland Basin from 2°W to 1°E at selected depths during the years 1993-2008.

close to the same temperature during all the years finally reaching more or less the same value in 2008. The average annual increase is 0.015°C y^{-1}.

In figure 5.13b a rapid decrease in salinity between the first and second year followed by a rapid increase can be seen. After the increase between 1994 and 1995 the changes in the salinity show a more even pattern with a slow increase from 1998 to 2001. In the following year there is a slight decrease in salinity before the increase continues untill 2007. In 2008 the salinity has decreased in all layeres and the three deepest layers have reached the same salinity. The least saline water can be found in the uppermost layer during the early 1990s, but from 1997 the least saline water is found in the deepest layer untill 2005 where the uppermost layer again is least saline. The most saline water is in general found in the two intermediate layers (2500 and 3000 m). In general the salinity has increased over the years with 0.001 y^{-1} in average.

Figure 5.13c shows few changes in density over the years with the exeption of a rapid decrease in 1994. In the early 1990s there are some differences between the layers, but from 1997 the three deepest layers have more or less the same density througout the time series. From 2001 the least dense water can be found in the uppermost layer which give a significant density difference between this layer and

the three deepest layers indicating a larger density gradient between 2000 m and 2500 m in the years after 2001. There is a slight increase in the average density of 0.003 kg m^{-3} y^{-1}.
In figure 5.13d the general trend shows a continuous decrease in the oxygen concentration for all layers. The lowest oxygen concentration is found in 2008 for most layers except the 2000 m layer which has its minimum in 2003. For the 1990s and the beginning of the 2000s the highest oxygen concentration can be found in the deepest layer while the lowest values are found at 2000 m. In 2003, 2000 and 2500 m show the same value and from 2005 onwards the uppermost layer has the highest oxygen concentration followed by the two deepest layers giving that the lowest oxygen concentration can be found in the 2500 m layer. The concentration differs somewhat between the layers. However, the deepest layers are close in concentration and show the same pattern of change for most of the years, especially from 1998. The largest changes in oxygen concentration happens in the deepest layer, 3500 m, which decrease from 7.20 ml L^{-1} to 6.85 ml L^{-1} over the years investigated. The average decrease in the oxygen concentration for all layer is -0.015 ml L^{-1} y^{-1}.

5.5 TS-diagram with oxygen concentration

To provide an opportunity to link the different water masses with the annual oxygen concentration over the transect, TS-diagrams have been made for each year (Fig. 5.14, Fig. 5.15, and Fig. 5.16) including oxygen concentration in each datapoint. In these diagrams data from the surface layer above 500 m are not included. In each TS-diagram boxes giving the characteristics of the different water masses are shown. The boxes have been made based on the water mass characteristics as defined in Tabel 2.1 (Schlichtholz and Houssais, 2002).
From historical observations one would expect that the main water masses in the centre of the Greenland Sea would be Arctic Intermediate Water (AIW) and GSDW. This is the case for the early 1990s where the GSDW and the AIW are the only water masses present. The increase in temperature and salinity seen in the deep layer over the periode investigated changes the characteristics of the GSDW leading to more and more datapoints falling into the box with NSDWc characteristics. At the end of the periode all the deep water has the characteristcs of NSDWc. The oxygen concentration in this water mass has the lowest values. The oxygen distribution shows an increase in concentration in the AIW from the early 1990s to the 2000s, while in the GSDW and NSDWc boxes the oxygen concentration remains fairly the same with only some minor annual changes. The oxygen concentration is slightly lower in the NSDWc box than the GSDW box in the years when water is present in both boxes. When no datapoints falls into the GSDW box the lowest oxygen concetration is found in the NSDWc box. The measurements from the upper layer falls into the AIW characteristics. From early 2000s a change can be seen in the distribution of the datapoints from the upper layer. More and more datapoints fall into the NSDWw box.

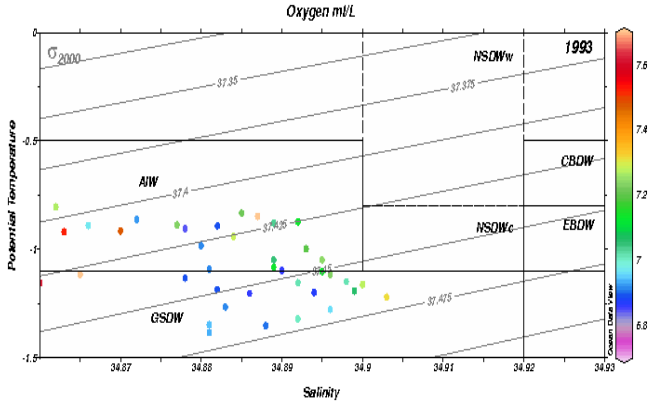

(a)

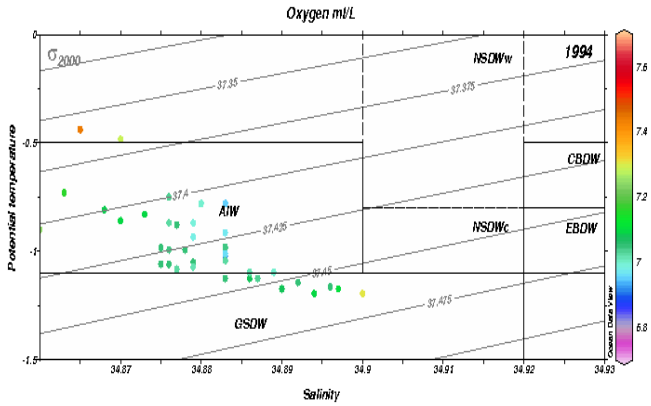

(b)

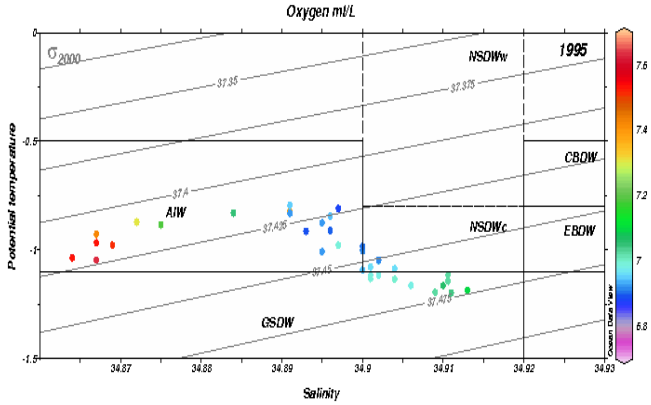

(c)

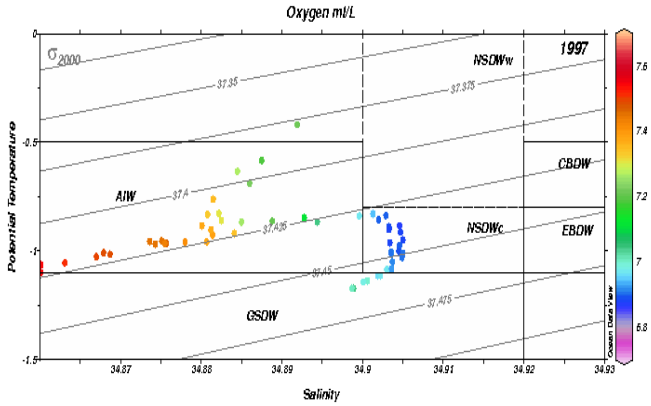

(d)

Figure 5.14: TS-diagram for each year with oxygen concentration (colour points). Adopted from Schlichtholz and Houssais, 2002.

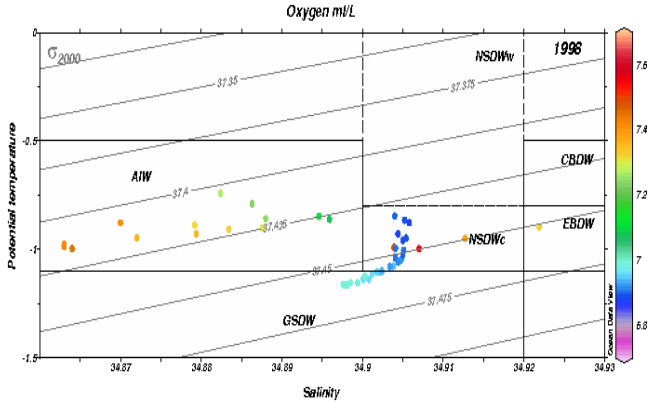

(a)

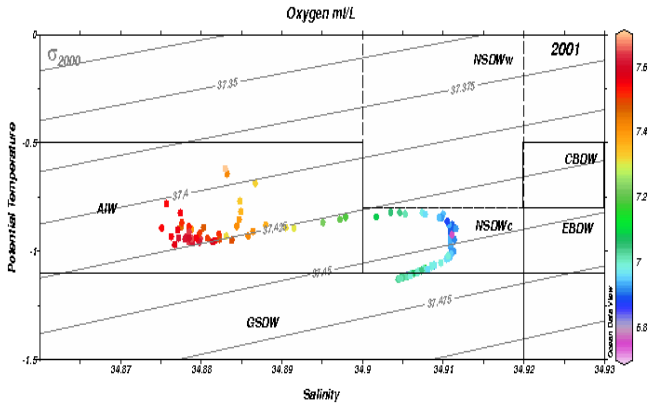

(b)

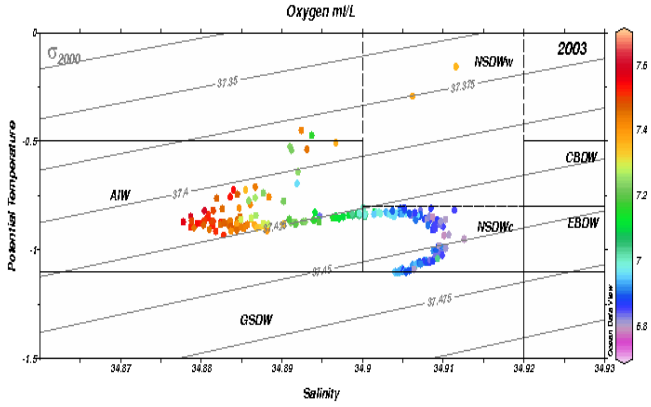

(c)

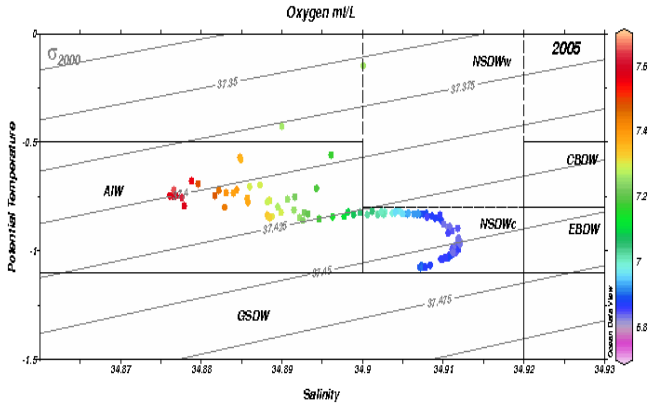

(d)

Figure 5.15: cont.: TS-diagram for each year with oxygen concentration (colour points).

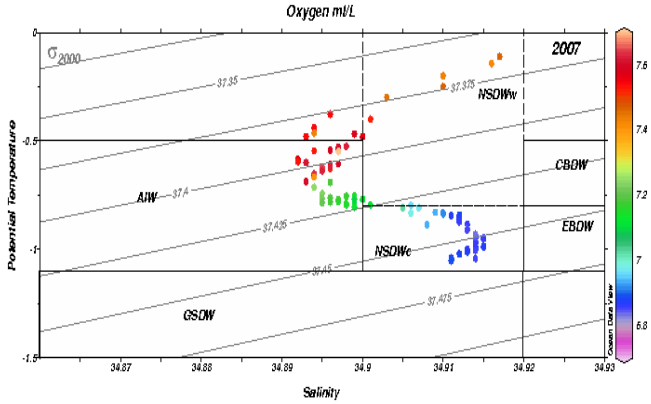

(a)

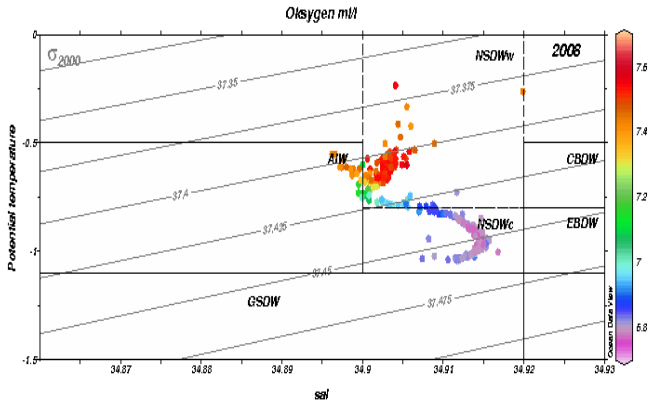

(b)

Figure 5.16: cont.: TS-diagram for each year with oxygen concentration (colour points).

5.6 Temperature maximum

Since the T_{max} layer is a prominent feature in the water column for most of the years this has been investigated in more detaile. The temperature, salinity, and oxygen concentration from the T_{max} layer have been sorted into time series together with the depth of T_{max} to easier investigate possible changes in this layer. The parameters have been taken from all station available on the transect and averaged to give a general view of this feature. The time series for all parameters along with the depth of the T_{max} are shown in Figure 5.17.
The temperature at the T_{max} shows an increasing trend over the 1990s and 2000s (Fig.5.17a) from -0.82°C to -0.75°C with the exception of a small spike in 1994. In the 1990s the salinity is increasing quite rapidly from 34.87 to 34.905, only abrupted by a minor decrease in 1998 (Fig.5.17b). During the 2000s the salinity remains at fairly the same value. For the oxygen concentration (Fig.5.17c) there are some variation over the years, but the general trend gives a decrease in concentration. In the early 1990s there is a rapid decrease followed by a rapid increase in 1998. From this year the oxygen concentration decreases over the remaining years. However,

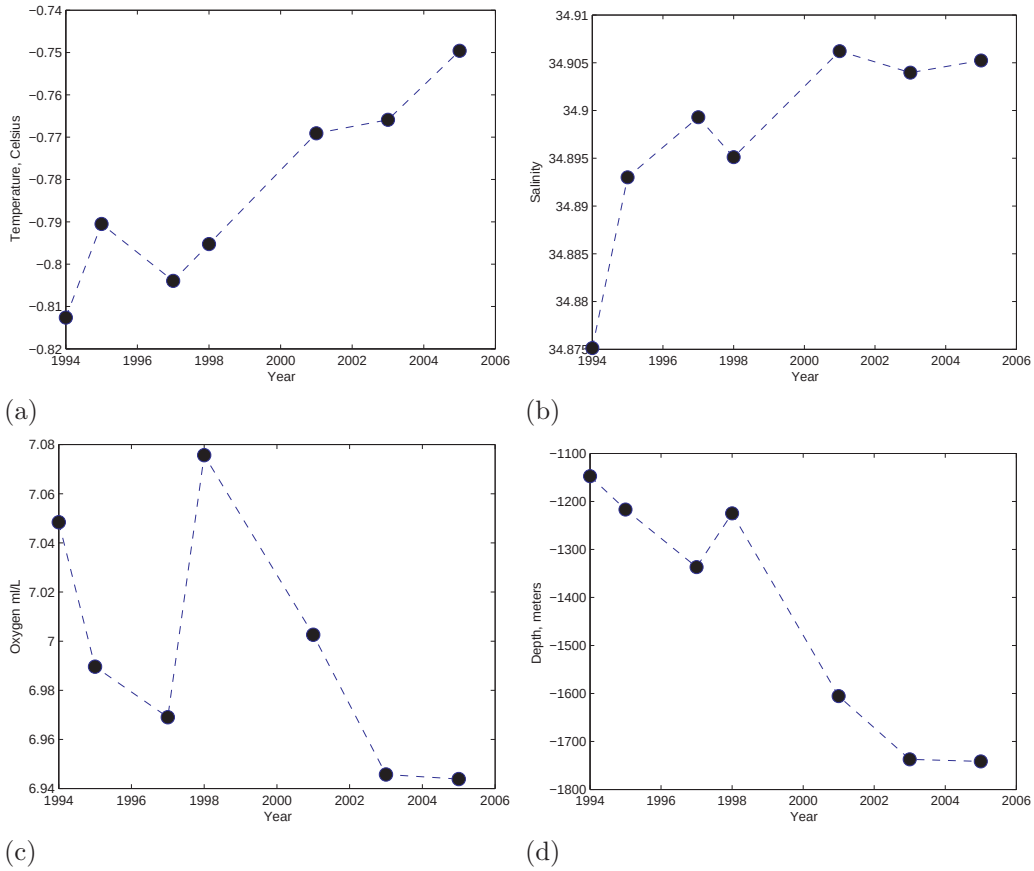

Figure 5.17: The temperature, salinity, and oxygen concentration in the T_{max} layer and the depth of T_{max}.

the decrease during the last years of the time series is very little. Over the years the depth of the T_{max} experience a decreasing trend starting at 1150 m in 1993 and ends up at 1750 m in 2005 (Fig. 5.17d).

Chapter 6

Summary & Discussion

During the years investigated there have been some significant changes in the Greenland Sea. The convection depth has reamined at intermediate depth over all the years investigated, but show a slow decending trend. In the deep layer there have been some interesting changes that probably are due to the combiantion of lacking deep convection and inflow of different water masses not originally present in the central Greenland Sea.

6.1 Zonally vertical sections

The main changes seen in the vertical sections presented in Chapter 5 were an increase in both temperature and salinity in the whole water column while there was a decrease in oxygen in the deep layer (Figs. 5.1, 5.2, 5.3, 5.4, 5.5, and 5.6). In the upper layer the oxygen concentration varies to some degree over the years with no obvious pattern. The most prominent change during the years is the increase of the vertical extent of the upper layer. In the deep layer the oxygen concentration shows a decreasing trend, as mentioned. Water that is not ventilated will experience a decrease in oxygen with time due to ongoing remineralization. There is also an increase in temperature and salinity indicating inflow of water masses with higher temperature and salinity than the GSDW had in the beginning of the 1990s.
In the upper layer there have been some changes during the years for all parameters with a continuous increase in temperature and salinity while the oxygen concentration show a more varying pattern. For the temperature and salinity the most significant changes seem to happen on the western rim of the Greenland Sea at 500-800 m depth where a inflow of warm and saline water can be seen. This inflow is probably the Return Atlantic Water flowing below the East Greenland Current carrying Atlantic Water recirculated in the Fram Strait. Even though this water mass has high temperatuer and salinity it is probably not the most significant contribution to the observed increase in temperature and salinity in the deep layer as it is assumed that the Atlantic Water would mainly pass around the central gyre in the upper layer (Rudels, 1986). The oxygen concentration variations from year to year are probably due to the changes in the strength of the winter convection, whereas the increase in vertical extent indicate that the convection is progressively

getting deeper in the water column over the years.
The changes seen in the deep layer are a continuation of the already observed increase in temperature and salinity in the 1980s (Aagaard et al., 1991). Aagaard et al. (1991) suggested that the increase in temperature and salinity was a result of mixing between GSDW and AODW (CBDW and EBDW), and that this increase was not compensated for by the effect of winter convection. Normally the deep convection would supply the Greenland Sea with cold low-salinity water and the observed increase in both temperature and salinity was thought to be the result of a shutdown of the deeep convection while the inflow of CBDW and EBDW continued. CBDW and EBDW had both higher temperature and salinity than the GSDW had originally in the beginning of their investigated time series. In the beginnig of the years investigated in this work the CBDW and EBDW also had higher temperature and salinity than the GSDW. From the zonal section plots these water masses can be seen in the deep layer as the salinity maximum values in a layer below the gradient and along the rim (e.g., Fig. 5.3 2003). In the temperature distribution the T_{max} layer is the only area which has the temperature characteristics of CBDW and EBDW indicating that this layer is a result of inflow of water from the Arctic Ocean along the rim of the Greenland Basin. These Arctic water masses can also be seen in the oxygen distribution (Fig. 5.5) as the oxygen minimas below the gradient and at the rim. The CBDW and EBDW have lower oxygen concentrations since these water masses consist of water that is older than the GSDW (AMAP, 1998). Old water is a water mass that has not been ventilated recently and is therefore deprived of oxygen. Input of these old water masses may contribute to a decrease in the oxygen concentration in the Greenland Sea.
If there were deep convective events in the Greenland Sea the water column would be ventilated and the input of low oxygen concentration water would be compensated for along with the temperture and salinity increase. However, the deep convection have been reduced in the Greenland Sea since the 1980s (GSP, 1990) and continued in this manner over the 1990s and 2000s (e.g., Karstensen et al., 2004; Ronski and Budéus, 2005a). Thus leading to a continued increase in temperature and salinity followed by the decrease in oxygen concentration.

6.2 Changes in the central part of the Greenland Sea

The changes and trends between 2°W and 1°E can be seen in the Hov-Möller diagrams (Fig.5.7). The location of the gradients shows a similar trend for all the parameters. The most prominent features in the diagrams are the T_{max} layer and the warming and salinification of the Greenland Sea, making it more homogeneous for these parameters. In the density distribution there are few changes and the gradient remains at fairly the same depth during all years. For the oxygen concentration the most prominent change is the slow descend of the gradient, and the decrease in the oxygen concentration below the gradient.
In the upper layer there is a pattern showing three high oxygen concentration

fields. The reason for these can be several since the upper layer may be influenced by annual changes as a result of convection, mixing and intrusion of water masses from the periphery of the Greenland Sea. Another possibility is that the pattern is a result of years without data and/or the interpolation method. The low salinity in 1994 may be caused by bad data giving too low values. The low density in the same year is a consequence of this low salinity. This low in salinity is more likely a result of bad data than due to natural causes. In the deep layer the changes are of smaller extent due to the isolation from the more rapidly changing upper layer. The changes seen in this layer are mainly due to inflow of water masses of Arctic origin coming from the currents along the rim of the Greenland Basin, which are advected and mixed into the Greenland Sea Deep Water as discussed in the previous section. Comparing the temperature and the oxygen distribution it can be seen that the oxygen minimum right below the gradient coincides well with the T_{max} showing that this is a warmer and older water mass than the surrounding water masses. This indicates that the T_{max} consists of older water probably of Arctic origin.

6.3 Convection depth

The convection depth can be identified by the use of different parameters where the most commonly used are temperature and salinity. Here the convection depth has been identified by the use of oxygen concentration. For all parameters the convection depth is defined as the depth of the gradient separating the newly ventilated upper layer from the quite homogeneous isolated deep layer. When comparing the depths of the different gradients (see figures in Appendix A) it can be seen that the oxygen gradient is somewhat shallower than the temperature and salinity gradients. The reason for this is that the oxygen profiles are Winkler data which have a much courser vertical measurement resolution than the other two parameters. Figure 5.8 shows that using the mentioned method of identification of convection directly on the Winkler data will underestimate the convection depth.

Part of this work has been to investigate if oxygen concentration can be used as a proxy for the identifcation of convection depth, and also see if it can give an answer to what type of convection took place. To identify the type of convection it is necessary to define the different types of convection. Ronski and Budéus (2005a, 2005b) investigated ways of identifying the type of winter convection and showed a time series of convection depths from 1994 to 2002. They were able to identify both the type and depth of the convective events for most years, but one year gave inconclusive results concidering the convection type.

The convection type called mixed layer deepening is cosistent with the first theory of winter convection suggested by Helland-Hansen and Nansen (1909). The surface becomes more dense due to heat loss to the atmosphere and when the stratification becomes unstable the surface layer mixes and becomes more homogeneous. The mixed layer deepening is a progressive event penetrating deeper down the water column with time as the stability of the water column is erroded due to further cooling. This convection type can be recognised by a thoroughly mixed layer without any small-scale fluctuations. For oxygen this mixed layer deepening can be applied

directly. A layer which has higher oxygen concentration than the deep layer and is well mixed with no or little small-scale structures can be said to be the result of a mixed layer deepening.
If the convection type is a plume convection the surface water will reach a point of much higher density and plume rapidly down the water column without mixing with the surrounding water. In this case the convection layer will not be well mixed and may have small-scale fluctuations. Applied to oxygen concentration this convection type can be identified by a layer that is not particulary mixed and may have small-scale structures. Also at the end of the convection depth there may be a higher concentration than in the layer above since the plume mixes very little with the surrounding water it passes by (Ronski and Budéus, 2005b).
From Figure 5.12 the type of convection can be identified by comparing the vertical structure of the oxygen profile and the oxygen concentration between successive years. During the winter 1993-1994 (Fig. 5.12a) a mixed layer deepening down to 500 m has taken place and through the following winter 1994-1995 (Fig. 5.12b) there has been a mixed layer deepening reaching down to 1000 m. The profiles in 1995 show an upper layer with high oxygen concentration which is well mixed, except for one station. As mentioned earlier, there are horizontal differences and the profile in 1995 showing no convection may be located on the outskirt of the main convection area. Compared to the profiles in 1994 there is no doubt that there has been a convective event this winter due to the significantly higher oxygen concentration that can only be achived through transport of water from the surface. However, that does not mean that years without increase in oxygen concentration did not experience convection (Budéus, personal communication). Ronski and Budéus (2005a) have also reached the assumption that the convective event through the 1994-1995 winter is of the type mixed layer deepening. During the winter 1997-1998 all profiles show small-scale fluctuations as well as the upper layer is not well mixed. In some of the profiles from both years a oxygen maximum can be seen at intermediate depth indicating the location of the plume. Ronski and Budéus (2005a) have reached the same assumption for this year as well. During the winter 2007-2008 (Fig. 5.12d) there has probably been a mixed layer deepening reaching down to 1600 m. In both years the upper layer is fairly homogeneous without any small-scale disturbances in the structure. There are some differences in the convection depth between the stations that is due to the horizontal differences.
By comparing the assumed convection depth based on the oxygen concentration profiles with the results from Ronski and Budéus it can be seen that there are some differences for most of the years (Fig.6.1). In 1995 the convection depth was 1100 meters according to Ronski and Budéus, while the oxygen profiles gave a convection depth of 1000 meters. The results from 1997 shows the same convection depth at 1100 m, while in 1998 Ronski and Budéus found the convection depth to be 900 m in contrast to the 1000 m given by the oxygen profiles. The last year that can be compared is 2001, where Ronski and Budéus found the convection depth to be 1400 m while the oxygen concentration showed a convection depth at 1200 m. The differences are mainly caused by the fact that they use CTD profiles while the oxygen profiles are from Winkler measurements. The best would have been to compare oxygen sensor data (Fig. 5.11), but these data start in 2003 and therefore

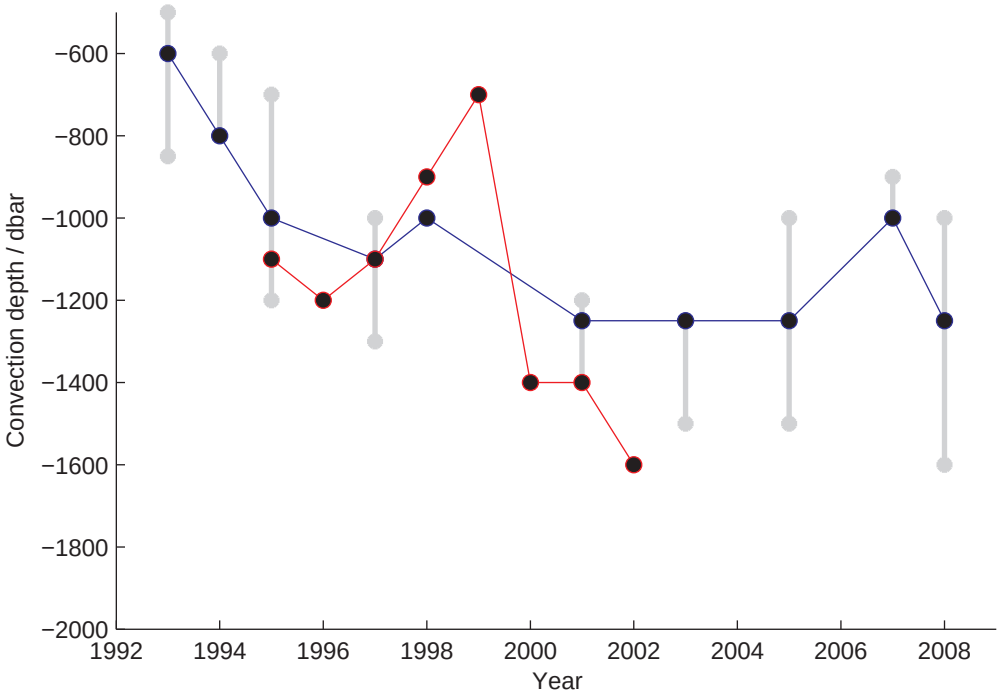

Figure 6.1: Convection depth from Winkler data (blue) compared to convection depth as described by Ronski and Budéus, 2005a (red).

do not coincide with their time series.

6.4 Changes in the deep layer

Since the 1980s the convective events in the Greenland Sea have been limited to the intermediate depths, and thereby not causing any particular deep water production (GSP Group, 1990). Because of this the deep layer has been investigated separatly to see if there are any changes than can be linked to this. To obtain a better view of the trends and changes in the deep layer four dephts have been selected for a more thorough inverstigation. The selected depths are as follows; 2000 m, 2500 m, 3000 m, and 3500 m.
The differences from year to year give a similar pattern in all the depths for most of the years (Fig. 5.13). The temperature and salinity experience an increase while the oxygen concentration decreases. The similar pattern in all the depths indicates that the changes happen throughout the deep layer. The 2000 m depth shows the greatest changes probably because this layer is closest to the depth of convection and are influenced by the ventilated upper layer to some extent. The influence by the ventilated layer can be best seen in the oxygen concentration (Fig. 5.13d). In the beginning of the time periode the 2000 m layer has the lowest oxygen concentration which probably is a result of the location of the oxygen minima below the gradient at approximately 2000 m for most years, but descending somewhat in the 2000s. In 2001 there is a much larger difference between the 2000 m layer and

the other layers. From Figure 5.6a it can be seen that there are quite high oxygen values in the deepest parts of the central parts. These high oxygen values can also be seen in the years before 2001 and are probably the remnants of the high oxygen concentration in the deep layer as a result of past deep convective events. As time passes the oxygen concentration in the deep layer sinks while the vertical extent of the ventilated upper layer increase, as already mentioned. This can also be seen in Figure 5.13d where the 2000 m layer has the highest oxygen concentration from 2003 onwards.
There are some years that show some differences from the trend. In 1994 there is a low salinity which can also be seen in the density followed by a high salinity where the three lowest layers all have the same value. These salinities may have natural causes such as inflow of fresh water due to sea ice melt causing a less saline water mass to mix down during convection. For the high salinity peak there may have been a winter with much ice formation prodcing highly saline brine that is transported into the deep layer due to convection. Another explanation may be that the measurements are not good giving data with erronuous values. This may be suspected as the temperature does not reveal any changes in the water mass as a result of ice melt or production. In 2001 there is a peak in oxygen concentration with probably too high values that may be due to natural or human causes. An increase in the oxygen concentration in the deep layers can only be caused by mixing with water from the surface layer. This is not probable as the transport of water from the surface layer depends on the convection and it is known that the convection has not penetrated beneath the intermediate layer during the years investigated. Therefore it is more likely that the high concentration is a result of human influence. Oxygen concentration measurements depend somewhat on the person making the measurement and thus there are potential for data to have too high or low values.

6.5 TS-diagram with oxygen concentration

The changes in the deep parts of the Greenland Sea during the years investigated have shown an increase in temperature and salinity along with a decrease in oxygen. A consequence of this is a change in the characteristics of the water masses present in the Greenland Sea as seen in Figures 5.14, 5.15, and 5.16.
The water masses present in 1993 are the Arctic Intermediate Water and the Greenland Sea Deep Water which are the water masses known to dominate the Greenland Gyre. However, due to the increase in temperature and salinity the characteristics of the GSDW becomes more and more similar to the NSDWc while some of the AIW becomes similar to NSDWw. During the years the amount of water with NSDWc characteristics increases while the amount with GSDW characteristics decreases. Looking at the TS-diagram it can be seen that the NSDWc lies between the GSDW and the EBDW, and the NSDWw lies between the GSDW and the CBDW. Mixing of EBDW and GSDW and CBDW and GSDW will produce a water mass with the characteristics of NSDWc and NSDWw, respectively. The TS-diagrams support the assumption that the changes seen in the hydrography of the Greenland Sea is a result of water flowing in from the Arctic Ocean where it

advects and mixes with the GSDW.
Investigations of the oxygen concentration in the TS-diagrams show that the concentration is decreasing and that the highest concentration can be found in the water with lowest density, as would be expected. The decreasing trend in oxygen concentration also support the theory that the changes in the Greenland Sea is due to inflow of water from the Arctic Ocean. The continued decrease in oxygen suggests that the water present in the Greenland Sea gets mixed with an older water mass. Deep water from the Arctic Ocean have a long residence time meaning that it remaines for many years in the basins before it continues to flow and are therefore old, as already mentioned. Without any deep convection in the future this increase in temperature and salinity, as well as the decrease in oxygen concentration, will not be counter affected and the trend will continue.

6.6 Temperature maximum

A prominent feature in the Greenland Sea for most of the years is the T_{max} layer at intermediate depth below the ventilated upper layer. The temperature maximum together with a deep salinity maximum shows the presence of the Arctic Ocean Deep Water in the form of EBDW and CBDW in the central parts of the Greenland Sea (Meincke et al., 1997). This layer is located right below the depth of the convection layer and thus it is interesting to se how it developes over the years.
The temperature and salinity in this layer (Fig.5.17) show the same increasing trend seen in the rest of the water column and can probably be attributed to the inflow of Arctic Water together with the lack of deep convection. As mentioned, the T_{max} lies right below the convection depth and is not influenced by addition of newly ventilated water. The exsistance of the temperature maximum indicate that there have not been a convection beyond this depth (Budéus et al., 1998) as the convection would deteriate this layer. The oxygen concentration (Fig. 5.17) has an overall decreasing trend consisting with the trends in the water column for all the parameters, but in 1998 and 2001 there are two peak values with much higher oxygen concentration. These peaks can not be seen in the temperature, but for salinity there is a decrease in 1998 along with a rise of the T_{max} layer depth. The increase in oxygen indicate that the T_{max} layer is affected by ventilated water as this is the only way for an increase in oxygen to take place at this depth. This is supported by the decrease in salinity since the freshest water is found in the surface layer. The high oxygen concentration in 2001 can be the remains of the peak in 1998. However, there may have been an influence of ventilated water that cannot be seen in the other parameters due to the increasing trends.

Chapter 7

Conclusion

The changes in the oxygen concentration during the investigated time period indicate that there have not been any convection reaching below the intermediate depth. Investigation of the convection depth showed that the Winkler profile underestimates the convection depth compared to the parameters measured by the CTD or oxygen sensor. With this in mind it is easy to conclude that the Winkler data should not be used to identify convection depth if oxygen sensor data are available. The latter give a good estimate of the loaction of the convection depth and should be used in stead.

The most prominent feature in the Greenland Sea is the temperature maximum located at intermediate depth close to the salinity, density, and oxygen concentration gradients. The characteristics of the T_{max} layer indicate that it is of Arctic origin. During the years the convection only reaches down to intermediate layer above the T_{max} probably causing the T_{max} to remain for several years. The T_{max} appeared in the upper layer in the beginning of the 1990s and descended down to 1800 meters depth before it disappeared in 2007. This disappearance of the T_{max} is not due to a convective event, but probably a result of the increase in temperature and salinity in the upper layer.

During the time period investigated the oxygen concentration in the deep layer of the Greenland Sea has decreased. The decrease in oxygen concentration is followed by an increase in temperature and salinity, indicating mixing of water masses of different origin than the Greenland Sea. The mixing water masses is assumed to be of Arctic origin, where the water masses have higher temperatures and salinities and a long residence times in their respective basins, meaning they have been isolated from the surface over a long period of time providing low oxygen concentration. If there were convective events during winter exeding the intermediate depth the GSDW would be supplied with cold, fresh newly ventilated water with higher oxygen concentration. The supply of such a water mass would counter act an increase in temperature and salinity, as well as a decrease in oxygen. The investigation based on the TS-diagrams reveals that the GSDW is changing into a water mass characteristic similar to the NSDWc. The shutdown of the deep convection has probably caused this change.

Chapter 8

Further work

In this work an attempt to correct the oxygen sensor was conducted. However, no clear answers were found to what would be the best way of performing the correction. Considering the convection depth and the hydrographic changes in the Greenland Sea there are still questions to be answered and different approaches that can be made in further investigation.

- Further investigations of sensor correction are necessary to be able to find one method that is supperior to the others. Suggestions for further investigatments are to divide the profile into intervals based on the bottle data points, or by using the sensor profile divided into smaller depth intervals to get a smoother structure.

- Another approach to the sensor correction may be to use the voltage when correcting, as suggested in SBE App. note no.64-2 (SBE, 2008b). In this note there is a correction suggestion that could be investigated to see if it provide a better way for sensor correction.

- In this work the ARK-cruises were the starting point and the Johan Hjort cruises were used to extend the time series. Since there is a possibility that some of the difference in the oxygen concentration is caused by human influence due to different routines when performing the Winkler titration, investigation of the oxygen concentration from the Johan Hjort cruises during the 2000s may provide a perspective on the difference between the cruises/institutes. If the oxygen concentrations are biased by the person performing the measurements such an investigation may give a better answer whether the observed changes in oxygen is real or a result of human influence.

- In the Greenland Sea there have been two known warming periodes during this century, one late in the 1950s and one in the late 1980s, and one cold period in the early 1970s. These periodes where discussed by Meincke (1991), who suggested a time period of 30 years, half the NAO index time period. It was also suggested that the cooling period where dominated by new production of GSDW and the warming period where dominated by mixing of the water masses around the Greenland Gyre. With this in mind, investigation of a longer time series along with comparison with the NAO index may make it

possible to give a statement whether or not the deep convection is part of an oscillating system as suggested by Meincke (1991).

Chapter 9

Referances

Arctic Monitoring and Assessment Programme, 1998: AMAP assessment report: Arctic pollution issues, Arctic Monitoring and Assessment Programme, Oslo, Norway, 3, pp. 69-72.

Aagaard, K., and E. C. Carmack, 1989: The role of sea ice and other fresh water in the Arctic circulation, J. Geophys. Res., 94(C10), 14485-14498.

Aagaard, K., E. Fahrback, J. Meincke, and J. H. Swift, 1991: Saline outflow from the Arctic Ocean: Its contribution to the deep waters of the Greenland, Norwegian, and Iceland Seas, J. Geophys. Res., 96(C11), 20, 433-20,441.

Blindheim, J., and F. Rey, 2004: Water-mass formation and distribution in the Nordic Seas during the 1990s, ICES Journal of Marine Science, 61, 846-863.

Blindheim, J., and S. Østerhus, 2005: The Nordic Seas main oceanographic features. In: The Nordic Seas: An integrated perspective, Geophysical Monograph Series 158, AGU 10.1029/158GM03.

Broecker, W. S., and T.-H. Peng, 1982: Tracers in the sea, Columbia University, Eldigo Press, Palisades, New York, p. 110.

Budéus, G., W. Schneider, and G. Krause, 1998: Winter convective events and bottom water warming in the Greenland Sea, J. Geophys. Res., 103(C9), 18513-18527.

Carmack, E. and K. Aagaard, 1973: On the deep water of the Greenland Sea, Deep-Sea Research, 20, pp. 687-715.

Carpenter, J. H., 1965: The Chesapeake Bay Institue technique for the Winkler dissolved oxygen method, Limnol. Oceanogr., 10, 141-143.

Clarke, R. A., J. H. Swift, J. L. Reid, and K. P. Koltermann 1990: The formation of Greenland Sea Deep Water: double diffusion or deep convection?

Deep-Sea Research, 37, No. 9, pp. 1385-1424.

Codispoti, L., 1988: One Man's Advice on the Determination of Dissolved Oxygen in Seawater, http://oceanweb.ocean.washington.edu/courses/oc201/OxygenProtocol.pdf.

GSP Group, 1990: Greenland Sea Project: A venture toward improved understanding of the oceans' role in climate, Eos Trens. AGU, 71, 750-751, 754-756.

Gytre, T., 2004: Havets oppløste oksygen - hvor kommer det fra og hvorfor er det så nødvendig?, Institute of Marine Research, Norway, www.imr.no/__data/page/4637/7.13_Tema_Havets_opploste_oksygen_-_hvor_kommer_det_fra_og_hvorfor_er_det_sa_nodvendig.pdf. (in Norwegian)

Helland-Hansen, B. and F. Nansen, 1909: The Norwegian Sea, Report on Norwegian Fishery and Marine-Investigations, 2, No. 2, pp. 323-330.

Karstensen, J., P. Schlosser, D. W. R. Wallace, J. L. Bullister, and J. Blindheim, 2005: Water mass transformation in the Greenland Sea during the 1990's, J. Geophys. Res., 110, C07022, doi: 10.1029/2004JC002510.

Meincke, J., 1991: Variability of Convective Conditions in the Greenland Sea, ICES C.M./C:14.

Meincke J., B. Rudels and H. J. Friedrich, 1997: The Arctic Ocean-Nordic Seas thermohaline system, ICES Journal of Marnie Scinece, 54, 283-299

Metcalf, 1955: On the transformation of bottom water in the Norwegian Basin, Trans. Am.geophys. Un., 36(4), 595-600.

Mohn, H., 1887: Nordhavets dybder, temperatur og strømninger, Den Norske Nordhavsekspedisjon 1876-1878 II, Grøndahl Forlag, Christiania, p.67.

Ronski, S., and G. Budéus, 2005a: Time series of winter convection in the Greenland Sea, J. Geophys. Res., 110, C04015, doi: 10.1029/2004JC002318.

Ronski, S., and G. Budéus, 2005b: How to identify winter convection in the Greenland Sea from hydrographic summer data, J. Geophys. Res., 110, C11010, doi: 10.1029/2003JC002156.

Rudels, B., 1986: The Θ-S relations in the northern seas: Implications for the deep circulation, Polar Research, 4, 133-159.

Sarmiento, J. L., and N. Gruber, 2006: Ocean biogeochemical cycles, Princeton University Press, pp.7-15, 181-186.

SBE, 2008a: SBE 43 Dissolved Oxygen Sensor - Background Information, Deployment Recommendations, and Cleaning and Storage, Application note no.64, http://www.seabird.com/application$_n$$otes/AN64.htm$.

SBE, 2008b: SBE 43 Dissolved Oxygen Sensor Calibration and Data Corrections using Winkler titration, Application note no.64-2, http://www.seabird.com/application_notes/AN64-2.htm.

SBE, 2009: Sea-Bird Dissolved Oxygen Sensor SBE 43, Specification brochure, http://www.seabird.com/products/spec_sheets/43data.htm.

Schlichtholz, P., and M. N. Houssais, 2002: An overview of the Θ-S correlations in the Fram Strait based on the MIZEX 84 data, Oceanologia 44(2), 243-272.

Schlitzer, R., Ocean Data View, http://odv.awi-bremerhaven.de, 2004.

Wadhams, P., J. Holfort, E. Hansen, and J. P. Wilkinson, 2002: A deep convective chimney in the winter Greenland Sea, Geophysical Research Letters, 29, 10, 1434.

Wilkinson, J. P., and P. Wadhams, 2003: A salt flux model for salinity change through ice production in the Greenland Sea, and its relation to winter convection, J. Geophys. Res., 108(C5), 3147.

Winkler, L. W. 1888: Die Bestimmung des in Wasser Gelösten Sauerstoffes, Berichte der Deutschen Chemischen Gesellschaft, 21, 28432855, doi:10.1002/cber.188802102122.

Østerhus, S., and T. Gammelsrød, 1999: The Abyss of the Nordic Seas is warming. Journal of Climate,12, 32973304.

List of Figures

List of Tables

Appendix A

Vertical profiles

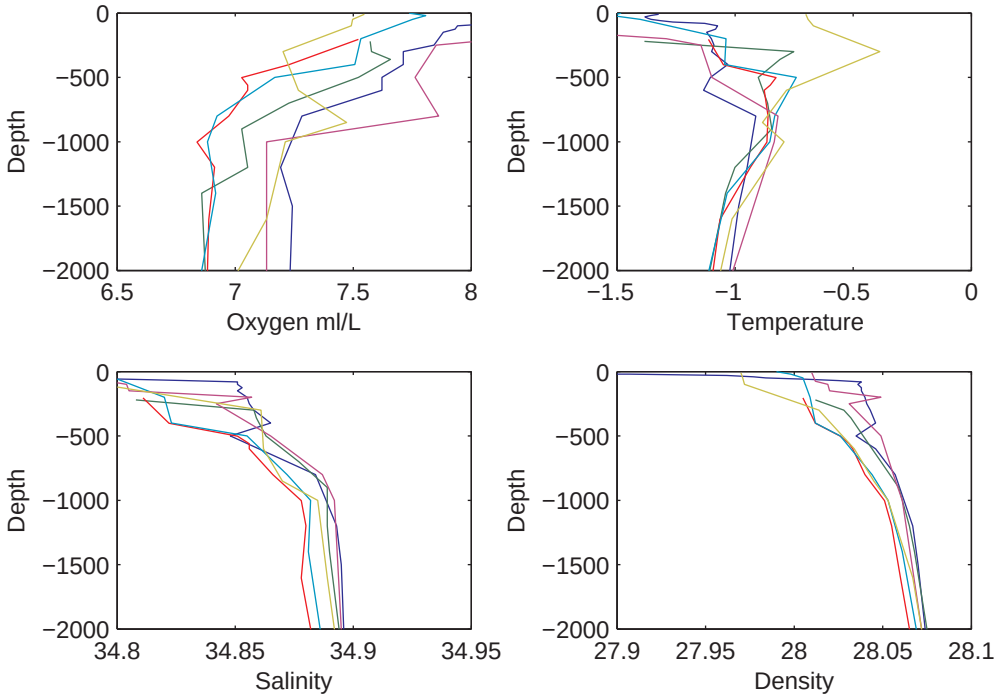

Figure A.1: Oxygen, temperature, salinity, and density profiles from the 75°N transect measured in 1993

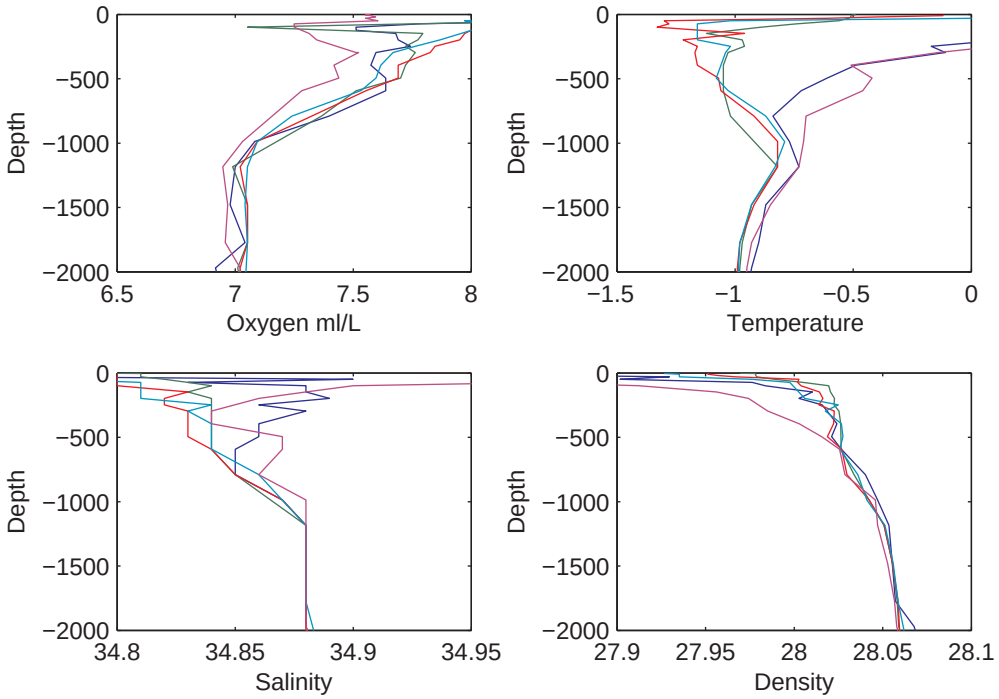

Figure A.2: Oxygen, temperature, salinity, and density profiles from the 75°N transect measured in 1994

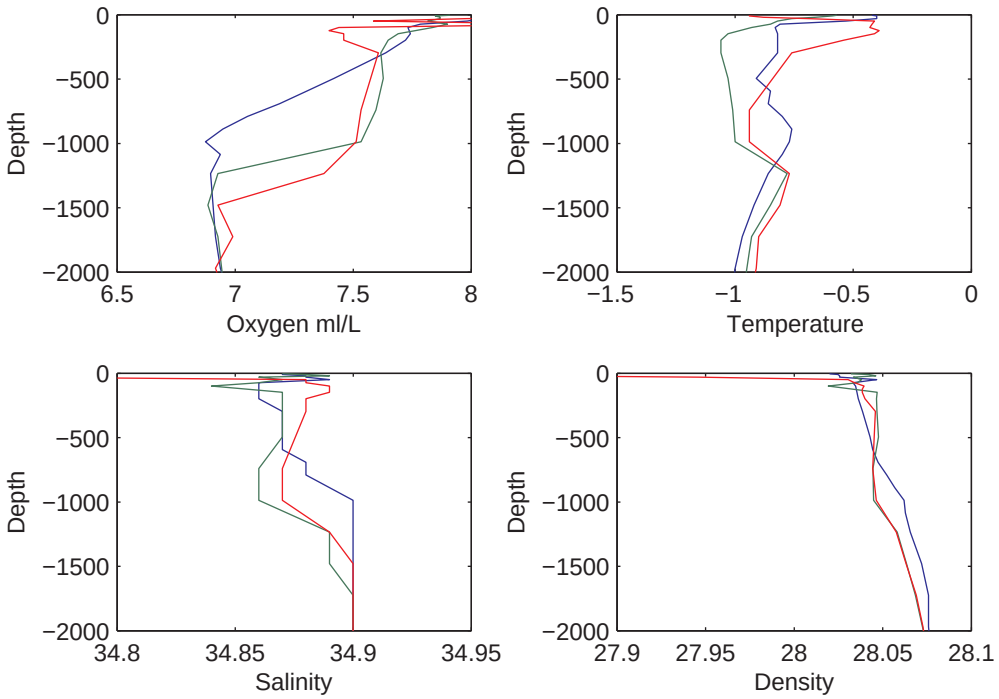

Figure A.3: Oxygen, temperature, salinity, and density profiles from the 75°N transect measured in 1995

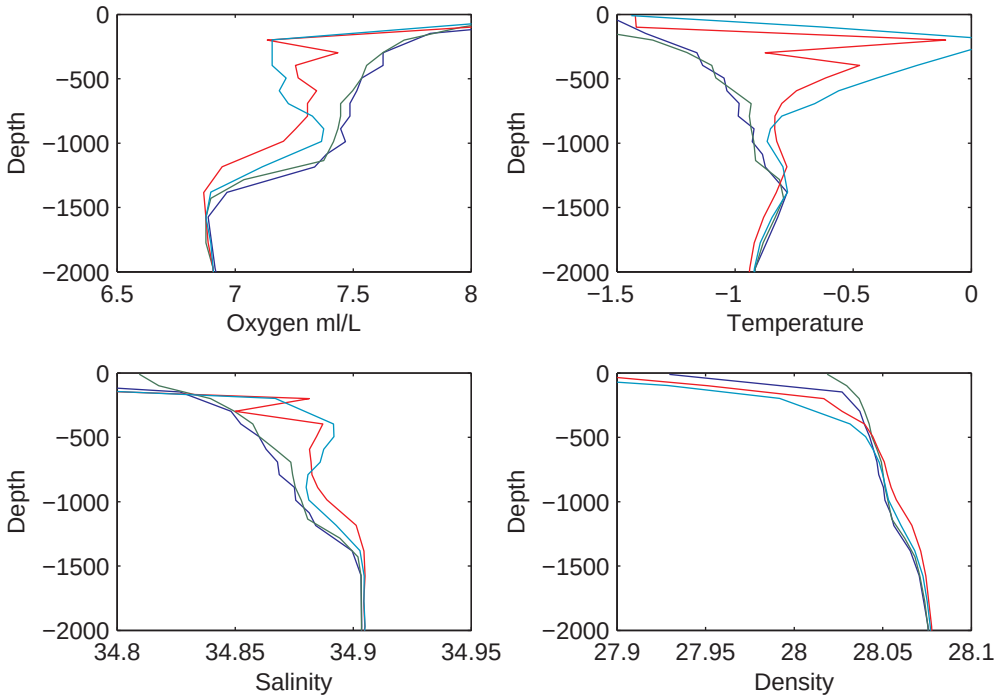

Figure A.4: Oxygen, temperature, salinity, and density profiles from the 75°N transect measured in 1997

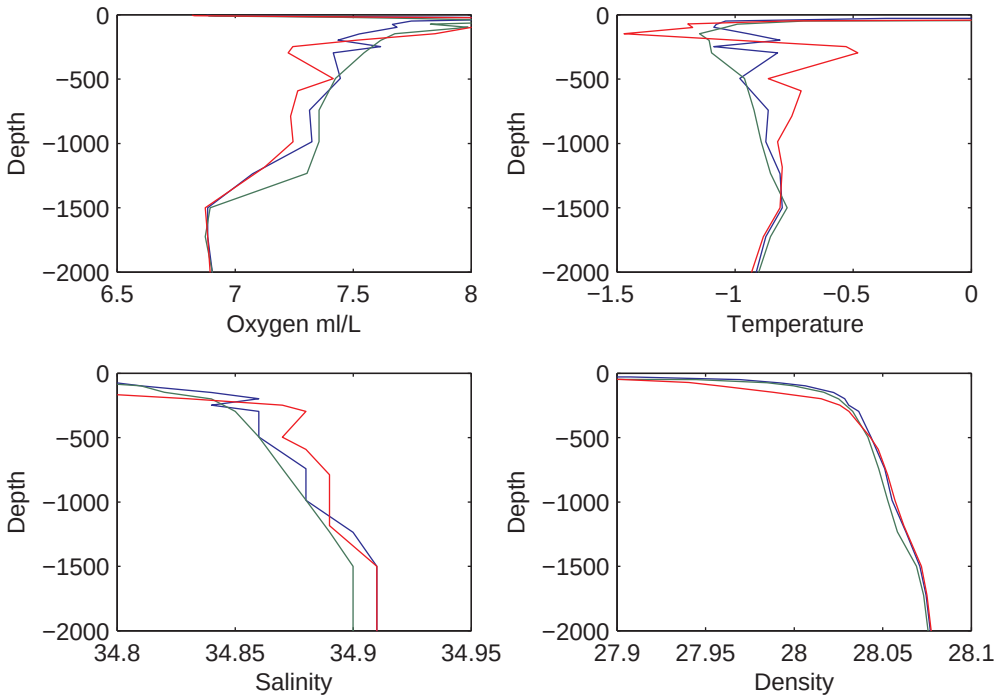

Figure A.5: Oxygen, temperature, salinity, and density profiles from the 75°N transect measured in 1998

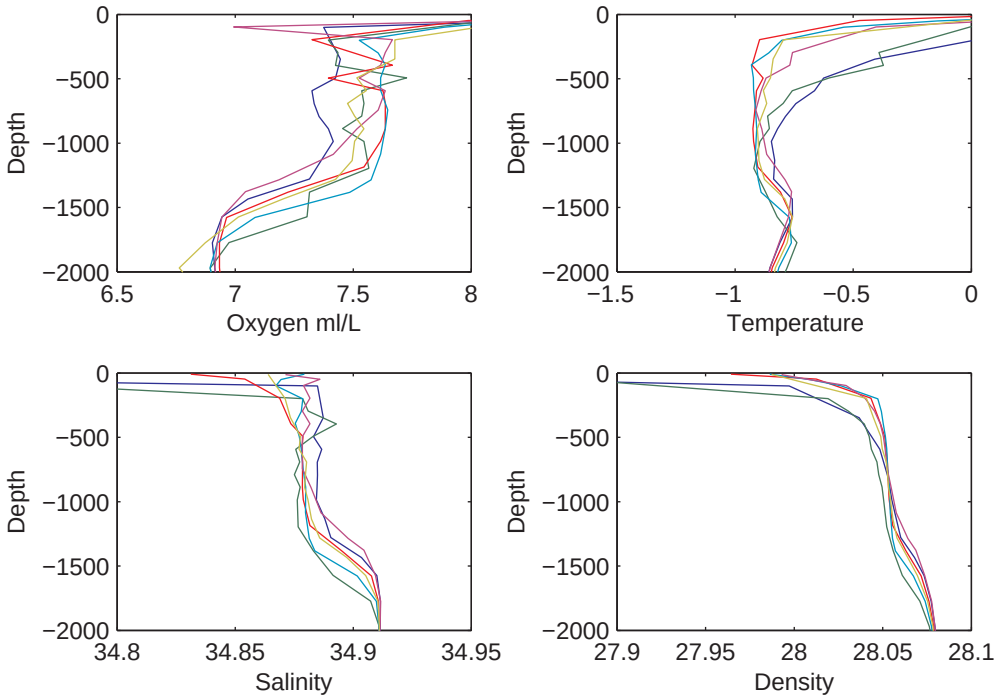

Figure A.6: Oxygen, temperature, salinity, and density profiles from the 75°N transect measured in 2001

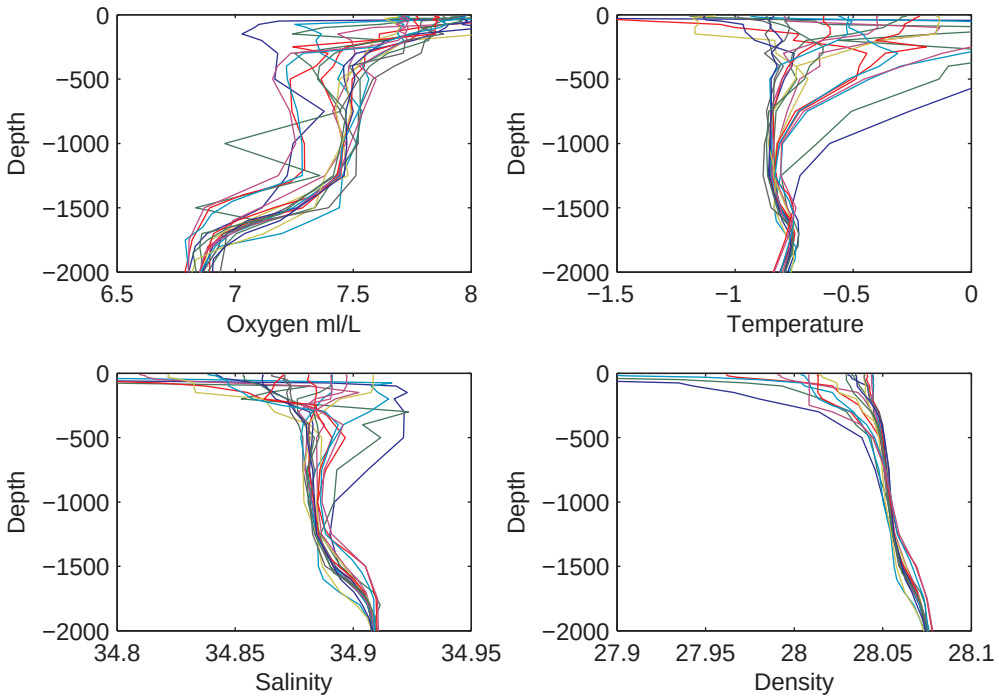

Figure A.7: Oxygen, temperature, salinity, and density profiles from the 75°N transect measured in 2003

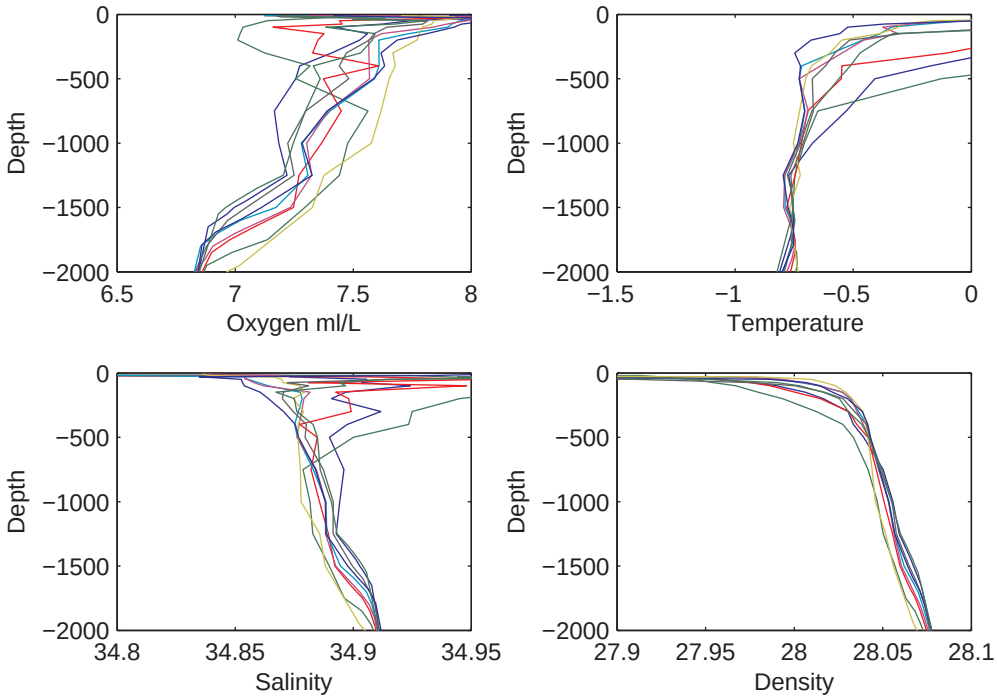

Figure A.8: Oxygen, temperature, salinity, and density profiles from the 75°N transect measured in 2005

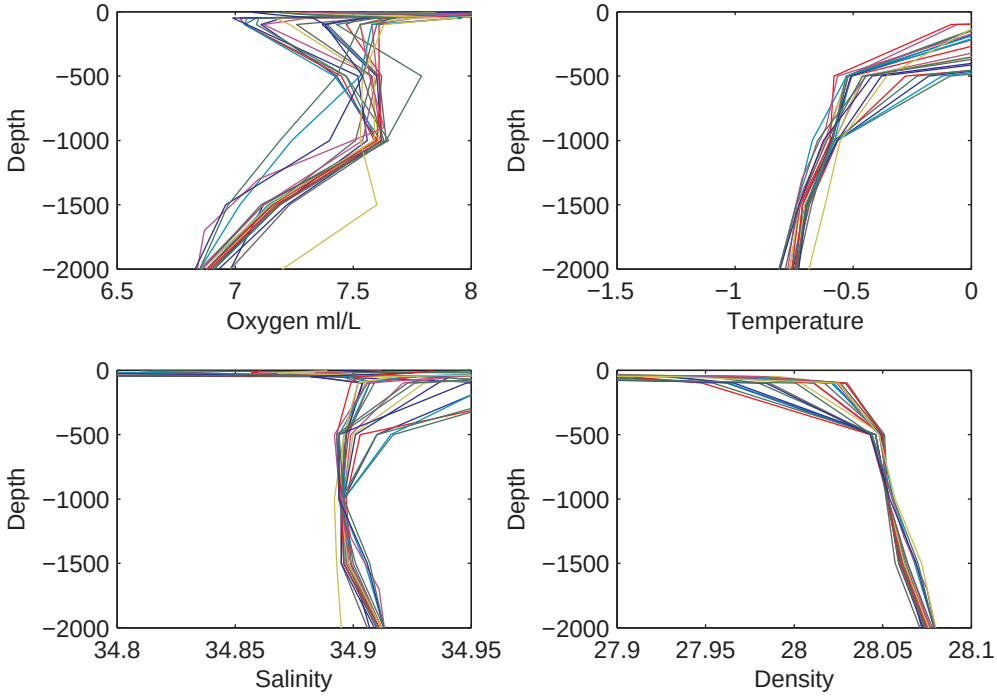

Figure A.9: Oxygen, temperature, salinity, and density profiles from the 75°N transect measured in 2007

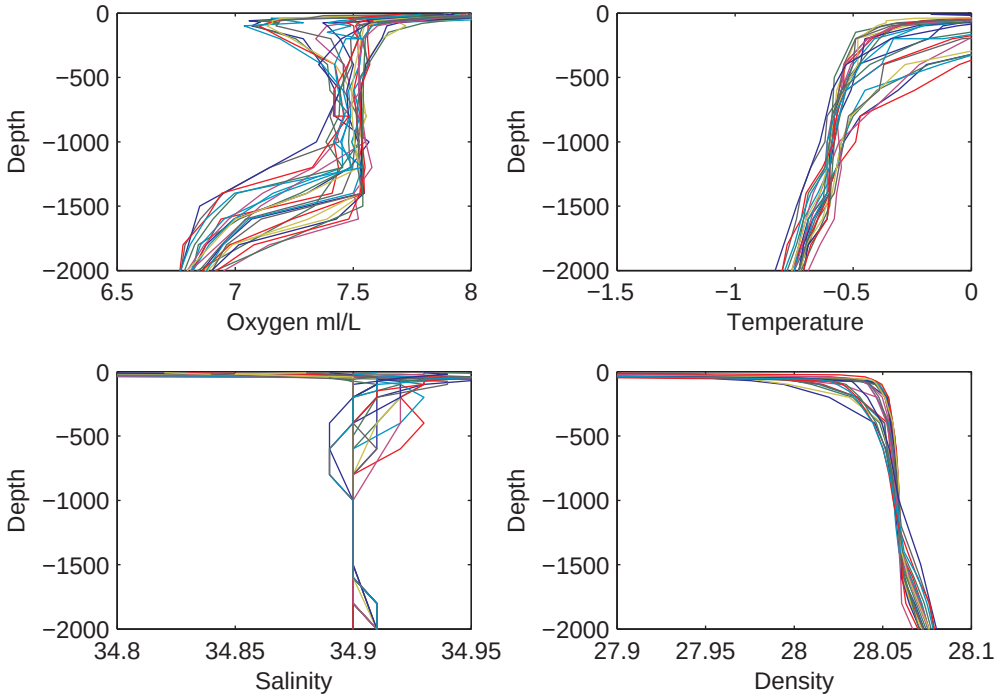

Figure A.10: Oxygen, temperature, salinity, and density profiles from the 75°N transect measured in 2008